

1 Article

## 2 S-layer Protein-based Biosensors

3 Bernhard Schuster <sup>1,\*</sup>

4 <sup>1</sup> Institute for Synthetic Bioarchitectures, Department of NanoBiotechnology, University of Natural  
5 Resources and Life Sciences, Muthgasse 11, 1190 Vienna, Austria; bernhard.schuster@boku.ac.at

6 \* Correspondence: bernhard.schuster@boku.ac.at; Tel.: +43-1-47654-80436

7 **Abstract:** The present Feature Paper highlights the application of bacterial surface (S-) layer proteins  
8 as versatile components for the fabrication of biosensors. One technologically relevant feature of  
9 S-layer proteins is their ability to self-assemble on many surfaces and interfaces to form a crystalline  
10 2D protein lattice. The S-layer lattice on the surface of a biosensor becomes part of the interface  
11 architecture, linking the bioreceptor to the transducer interface, which may cause signal  
12 amplification. The S-layer lattice as ultrathin, highly porous structure with functional groups in a  
13 well-defined special distribution and orientation and an overall anti-fouling characteristics can  
14 significantly raise the limit in terms of variety and ease of bioreceptor immobilization, compactness  
15 of bioreceptor molecule arrangement, sensitivity, specificity, and detection limit for many types of  
16 biosensors. The present paper discusses and summarizes examples for the successful  
17 implementation of S-layer lattices on biosensor surfaces in order to give a comprehensive overview  
18 on the application potential of these bioinspired S-layer protein-based biosensors.

19 **Keywords:** biosensor; S-layer protein; crystalline 2D protein lattice; lipid membrane platform;  
20 linking matrix; bioreceptor; biomimetics

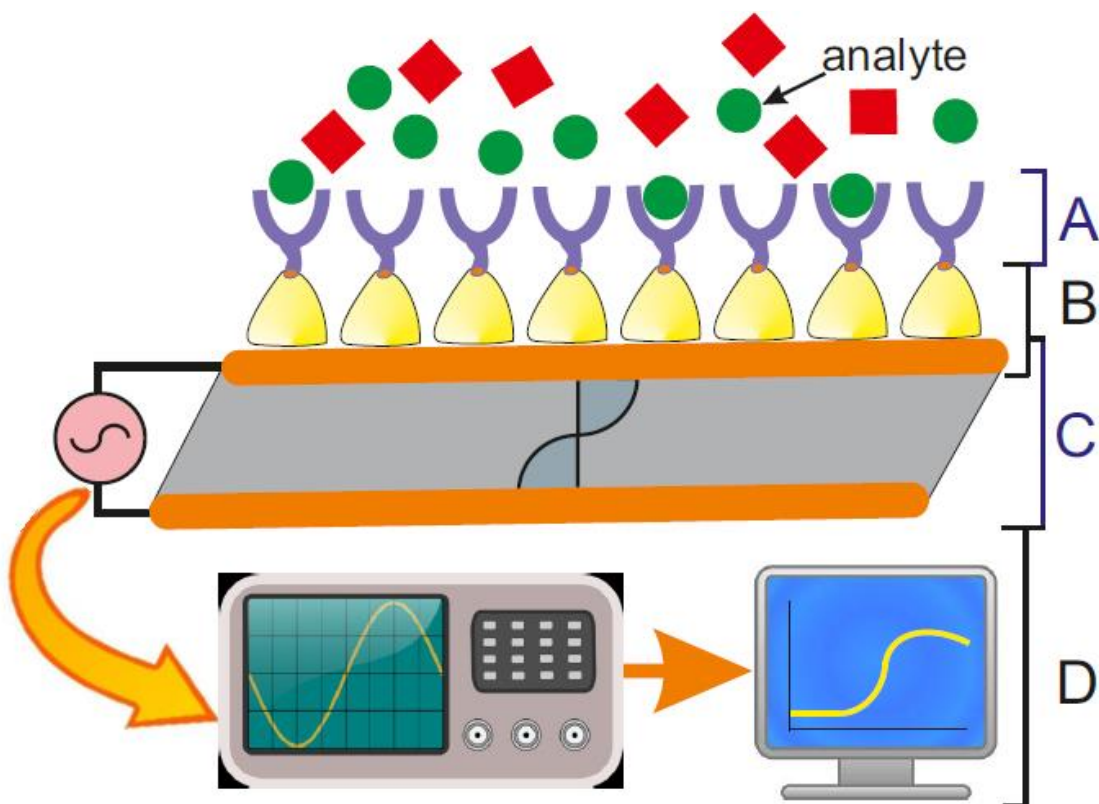
21

---

### 22 1. Introduction

23 Biosensor-related research has made tremendous progress over the past four decades, because  
24 the advance in electronics, nanolithography, nanobiotechnology, biomimetics and synthetic biology  
25 led to successful routes for combining biological systems with silicon technology. Biosensors are per  
26 definition devices, which use a biological recognition element retained in direct spatial contact with  
27 the transduction system [1] or, in simplified terms a device, that converts a physical or biological  
28 event into a measurable, mostly electrical signal [2]. Biosensors comprise in general of (Figure 1):

29 A) a biosensing element or bioreceptor, to which the analyte has a highly specific binding affinity.  
30 B) an interface architecture, which provides an environment for the proper functioning of the  
31 biosensing element and where the specific biological event, which gives rise to a certain physical  
32 phenomenon takes place.  
33 C) a transducer converting the physical phenomenon or chemical response resulting from the  
34 analyte's interaction with the biological element (e.g., physicochemical, optical, piezoelectric,  
35 electrochemical, etc.) into electrical signals. The latter can be reproducibly measured, quantified and  
36 processed [3].  
37 D) an associated electronics comprising of signal amplifier, signal processor and an interface like a  
38 display, which finally allows a user-friendly visualization and evaluation of the data [4].



39

40 Figure 1: Elements and selected components of an S-layer protein-based QCM-D biosensor. A) A  
41 biosensing element or bioreceptor comprising of accessible functions like, e.g., an antibody to which  
42 the analyte binds with highly specific affinity. B) An interface architecture comprising of a QCM-D  
43 sensor surface covered by a recrystallized S-layer lattice, which provides an environment for the  
44 proper functioning of the biosensing element. Here the specific biological event takes place, which  
45 gives rise to a certain physical phenomenon. C) A transducer converting the physical phenomenon  
46 (piezoelectricity) resulting from the analyte's interaction with the biological element into an electrical  
47 signals. D) Associated electronics comprising of signal amplifier, signal processor and a display  
48 allowing a user-friendly visualization and evaluation of the data.

49 The biosensing element or bioreceptor is frequently a biologically derived or biomimetic  
50 material like living cell, tissue, enzyme, membrane protein (e.g., ion channel, receptor, pore-forming  
51 protein), membrane-active peptide (e.g., ionophore), antibody, nucleic acid, and biological sensitive  
52 elements created by genetic engineering. The analyte, which binds in a highly specific manner to the  
53 bioreceptor may be amongst others ions, nucleic acids and other organic molecules from cell cultures,  
54 human (blood, urine, saliva, tears, sperm, various secretions, etc.,) and food samples, and pollutants  
55 from environmental samples (e.g., air, water, soil, vegetation).

56 One of the most challenging tasks is to converge biological or biomimetic systems with silicon  
57 technology in order to generate the functional interface architecture [5]. Biological molecules may  
58 aggregate or even denature on the surface of electrodes, sensors or other mostly inorganic solid  
59 supports and hence, loose their function. In order to prevent the loss of function, very frequently an  
60 intermediate layer is generated in-between the biosensing element and the inorganic surface of (ion-  
61 sensitive) field-effect transistors, (interdigitated) microarray electrodes, metal-, polymer- or  
62 graphene-coated sensor chips, etc. This intermediate layer comprises either of polymers (e.g.,  
63 polyethylene glycol, chitosan, agarose, hydrogel, or polyelectrolyte) [6, 7], self-assembled monolayers  
64 (SAMs; e.g., alkanethiol, dialkylsulfides, silanes, phosphonates) [8-11], or a monomolecular array of  
65 self-assembled protein subunits forming surface layers (S-layers) [12-16]. If a lipid membrane is  
66 desired as part of the biosensing element, an incomplete layer of so-called tether molecules replace  
67 the rigid SAM [17-19]. Incomplete it the sense that one wants to have only few tether molecules,  
68 which anchor the membrane to the surface. This arrangement, where the tether molecules are mixed

69 with so-called spacer molecules ensures a certain retained fluidity of the lipid membrane [18]. The  
70 latter is very important if one wants to functionally reconstitute integral membrane proteins and/or  
71 membrane-active peptides in a tethered membrane. In general, a tether molecule is composed of a  
72 binding group to be anchored on a solid support (thiol, silane, chelation of Ni-ions with nitrilotriacetic  
73 acid, biotin, etc.), a hydrophilic backbone and a hydrophobic moiety to anchor the lipid membrane  
74 (alkyl chains, cholesterol, etc.) [20, 21]. Molecules like polymers (in particular polyethylene glycol),  
75 glyco-polymers, peptides and proteins are used so far to build up the hydrophilic part of the tether  
76 layers [22-24]. The challenge generating the intermediate layer is to combine multiple functions  
77 including: 1) to act as immobilization layer with a suitable binding to both, the inorganic support and  
78 the biological molecules (e.g., bioreceptors, matrix-forming lipids; 2) to allocate a binding matrix  
79 where immobilized molecules are arranged in a well-defined spatial and directed orientation; 3) to  
80 provide a reservoir for water and ions; and 4) to provide sufficient space and stability for the  
81 biosensing elements.

82 Moreover, some biosensors require an immobilization process of the bioreceptor to the sensor  
83 surface (metal, metal oxide, glass, polymer and other materials) using physical or chemical  
84 techniques [25]. This is in particular the case if one wants to rely on membrane proteins and  
85 membrane-active peptides as biosensing element because these biomolecules need a lipid membrane  
86 to adopt their functional structure and to deploy amplification properties. The immobilization of the  
87 biosensing element has the additional advantage to be assessable with the broad arsenal of surface-  
88 sensing techniques. Indeed, many biosensors rely on surface-sensitive techniques like surface  
89 plasmon spectroscopy (SPR) [26-28], surface acoustic wave (SAW), quartz crystal microbalance with  
90 dissipation monitoring (QCM-D) [29-32], electrochemical impedance spectroscopy (EIS) [33-36],  
91 cyclovoltammetry (CV) [37-39] or total internal reflection fluorescence microscopy (TIRFM) [40] as  
92 transducer. Important questions in this context are how one can create an intermediate layer with all  
93 the intrinsic properties listed above and how can the biosensing element be coupled to or integrated  
94 in this functional layer.

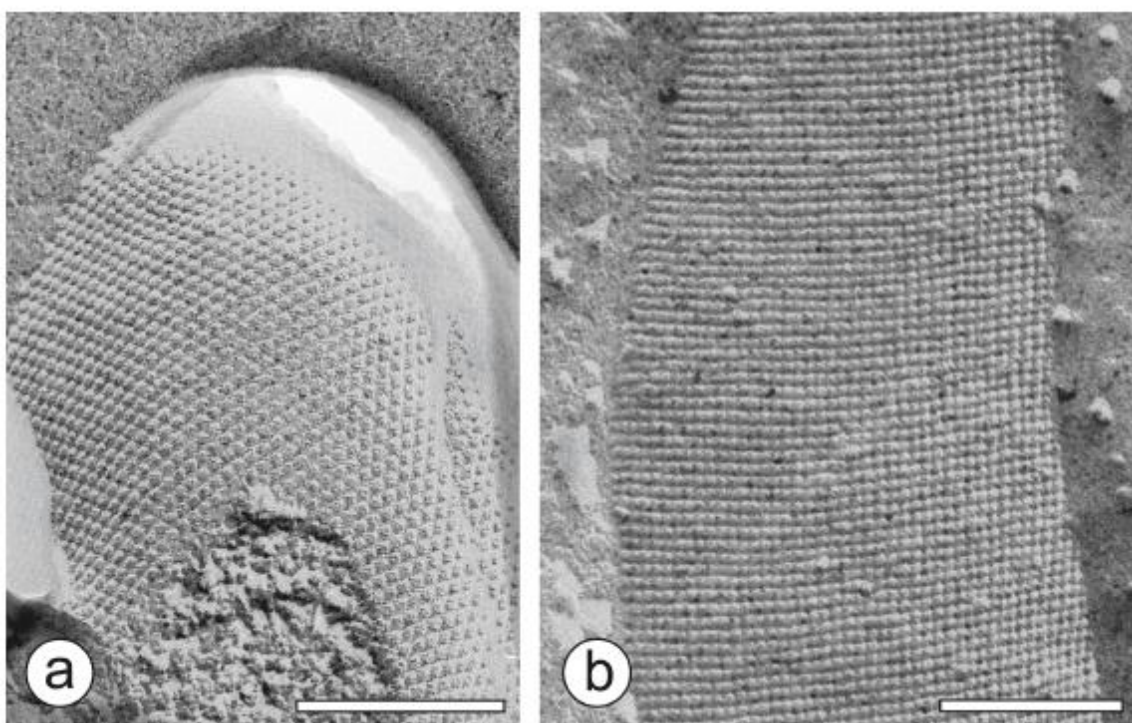
95 The present Feature Paper focusses on a promising approach to generate a particular type of  
96 protein-based intermediate layer, the so-called surface (S-) layer [41]. In the following, I present an  
97 introduction to bacterial S-layer proteins and their use for the immobilization of functional molecules  
98 and lipid membranes. Moreover, I also introduce S-layer fusion proteins and their utilization as  
99 components for the generation of biosensors. Finally, I discuss the application of S-layer lattices for  
100 the generation of functional lipid membrane platforms in detail and possible future directions for the  
101 application of these S-layer lattices in general are considered.

## 102 2. Bacterial S-layer proteins

103 The S-layer is defined as a “two-dimensional array of proteinaceous subunits forming the  
104 surface layer on prokaryotic cells” (Figure 2) [15]. They are found as outermost structure in hundreds  
105 of different species of almost every taxonomic group of walled bacteria and are an almost universal  
106 feature of archaea [15, 42-44]. As S-layers account for approximately 10% of cellular proteins in  
107 bacteria and archaea and since the biomass of prokaryotic organisms surpass the biomass of  
108 eukaryotic organism [45], S-layers can be considered as one of the most abundant biopolymers on  
109 Earth [15, 46]. Moreover, S-layers also represent the simplest biological protein or glycoprotein  
110 membranes developed during evolution [43, 47, 48].

111 High-resolution transmission electron microscopy (TEM) and atomic force microscopy (AFM)  
112 studies on the mass distribution of S-layer lattices revealed not only that the S-layer cover the entire  
113 cell surface as coherent layer [49-52], but demonstrated also the elegancy of these proteinaceous  
114 supramolecular bioarchitectures (Figure 2) [53]. Most S-layers are monomolecular assemblies of  
115 single subunit species with a molecular weight ranging between 40 kDa to 200 kDa. In general,  
116 bacterial S-layer lattices exhibit oblique (p1, p2), square (p4) or hexagonal (p3, p6) space group  
117 symmetry with a centre-to-centre spacing of the morphological units of 3.5 to 35 nm [42, 54, 55].  
118 Bacterial S-layers are generally 5 nm to 10 nm thick and reveal a rather smooth outer and a more  
119 corrugated inner surface. Furthermore, the S-layer lattice SbpA from *Lysinibacillus sphaericus* CCM

120 2177 showed an outstanding antifouling characteristic of in the presence of highly concentrated  
121 protein solutions (e.g., 70 g L<sup>-1</sup> human serum albumin), plasma and whole blood samples [56]. This  
122 finding is explained by the inherently (zwitterionic) neutral charge of the outer surface of SbpA.  
123 Moreover, S-layers are highly porous protein lattices (30% to 70% porosity) with pores uniform in  
124 size and morphology in the dimension of 2 nm to 8 nm [57-59]. Interestingly, many S-layers possess  
125 two or even more distinct classes of pores [42, 54, 55, 60, 61].



126  
127 Figure 2: TEM image of a freeze-etched and metal shadowed preparation of (a) an archaeal cell (from  
128 *Methanocorpusuculum sinense*), and (b) a bacterial cell (from *Desulfotomaculum nigrificans*). Bars, 200  
129 nm. Adopted from [15], copyright (2014) with permission from John Wiley & Sons Ltd.  
130

131 A little is known about the specific biological functions of S-layers but it is now recognized that  
132 they can function as protective coats against, e.g., bdellovibrios, bacteriophages, and phagocytosis;  
133 can act as molecular sieve, molecule and ion traps; promoters for cell adhesion; immune-modulators;  
134 surface recognition; antifouling coatings; and virulence factors in pathogenic organisms [15, 58, 62,  
135 63]. Moreover, the S-layer lattice is involved in the determination of cell shape and as a structure  
136 aiding in the cell division process in archaea, which possess S-layers as the exclusive envelope  
137 component external to the cytoplasmic membrane [64, 65]. Interestingly, ion-gating properties of  
138 microbial S-layer protein arrays have also been determined for the S-layer of *Deinococcus radiodurans*  
139 [66]. Ion transport appears to be mainly due to an electrical gradient inside the pores, presuming to  
140 originate from the negative charges present on this S-layer lattice. By evaluation of the gating  
141 characteristics of this nanoporous membrane toward various ionic species it turned out, that  
142 immobilized S-layers undergo a strong interaction with cations, in particular Ca<sup>2+</sup>-ions.  
143

144 One very important feature of S-layer proteins is the capability of isolated native or  
145 recombinantly produced subunits to self-assemble on surfaces or interfaces into crystalline arrays.  
146 These surfaces include glass, silicon oxide and nitride, mica, noble metals like gold, titan, platinum,  
147 but also stainless steel or many polymers as polystyrene, polyester, and cellulose, and on technically  
148 relevant materials like highly oriented pyrolytic graphite, graphene, or indium tin oxide [56, 67]. TEM  
149 [68-70] and AFM [71-73] are the most appropriate techniques to elucidate the recrystallization process  
150 of S-layer proteins. Crystal growth at interfaces (e.g., solid supports, air-water interface or lipid  
151 membranes) is initiated simultaneously at many randomly distributed nucleation points, and  
proceeds in plane until the crystalline domains meet, thus leading to a closed, coherent mosaic of

152 individual, several micrometers large S-layer patches [71, 74-76]. The growth of extended S-layers  
153 patches is favoured at low monomer concentrations due to the corresponding low number of  
154 nucleation sites. The individual patches are monocrystalline and separated by grain boundaries [71].

155 The formation of a coherent crystalline lattice depends on the used S-layer protein species, the  
156 environmental conditions of the subphase (i.e., ionic content and strength, pH-value) and on the  
157 surface properties of the interface. Interestingly, S-layer lattice can exhibit against cells in tissue  
158 cultures either cell adhesive (cytophilic) or cell repulsive (cytophobic) surface properties depending  
159 whether the inner or outer side, respectively, is exposed to the aqueous environment. The different  
160 orientation and function of the S-layer protein can simply be achieved by altering the recrystallization  
161 protocol from a basic (pH 9; resulting in an exposed outer, smooth cytophobic side) to an acidic (pH  
162 4; resulting in an exposed inner rough, cytophilic surface pattern) condition [77].

163 While the reassembly of S-layer proteins at the air-water interface and at planar lipid films is  
164 well defined [69, 70, 78-80], the deliberate modification of the surface properties of a solid support  
165 allows to specifically control the reassembly process [71, 75, 81-83]. For example, the S-layer protein  
166 SbpA, which is currently one of the most detailed studied S-layer proteins for functionalizing solid  
167 supports, forms monolayers with a height of 9 nm on hydrophobic surface and double layers on  
168 hydrophilic silicon supports [71]. The height of the double layer structure is 15 nm indicating that the  
169 two layers are resting on each other like two interdigitated-toothed racks. Furthermore, in  
170 comparison to hydrophilic surfaces, the layer formation is much faster on hydrophobic supports  
171 starting from many different nucleation sites and thus, leading to a mosaic of small crystalline  
172 domains (2D powder) [47].

173 In general, the S-layer is on the one hand side utilized as very precise immobilization matrix to  
174 present various biomolecules including bioreceptors in a unique manner [15, 84, 85]. On the other  
175 hand side, this protein-based intermediate layer constitutes also a versatile base plate for the  
176 generation of supported lipid membranes, which provide the essential environment for the  
177 reconstitution of functional membrane proteins and membrane-active peptides [41, 86, 87].

178 Although native S-layer proteins have already demonstrated their great potential as patterning  
179 elements and nanoscale building blocks, genetic approaches have opened up the possibility of  
180 modifying and tuning the natural properties of S-layer proteins [88, 89]. However, one has to take  
181 care that the S-layer proteins with inserted or fused foreign domains or proteins do not lose their  
182 capability to assemble into geometrically well-defined layers. The most relevant advantages of  
183 genetically engineered S-layers over less nanostructured approaches are the periodicity of functional  
184 domains in the nanometer range on the outermost surface of the S-layer lattice. To date, S-layer fusion  
185 proteins are produced through homologous expression and secretion by cells or inside a host  
186 organism, which is mostly *Escherichia coli* [89, 90]. Both strategies are suitable to produce bio-inspired  
187 materials with designed functional properties. Moreover, the possibility to fuse single or  
188 multifunctional domains of other proteins to S-layer proteins has led to a broad spectrum of  
189 applications ranging from fluorescent biomarkers, immobilized biocatalysts, vaccine, diagnostics,  
190 and sensor development, to biosorption of heavy metals and nanoparticle arrays [15, 50, 91, 92]. In  
191 this context, it is interesting to note that S-layer proteins may also be genetically engineered in order  
192 to introduce domains for the covalent binding of lipid molecules and thus, enhancing the stability of  
193 the entire composite S-layer supported lipid membrane (SsLM) [93-97]. Finally, the co-  
194 recrystallization of different S-layer fusion proteins will lead to a high flexibility for the variation of  
195 functional groups within a single S-layer array.

### 196 3. Modified S-layers as components in biosensors

197 Since S-layers represent one of the few examples in Nature, where proteins reveal the intrinsic  
198 capability to self-assemble into monomolecular lattices a considerable potential in biological and non-  
199 biological applications is evident. Previous studies demonstrated that S-layers represent an ideal  
200 patterning element for nanobiotechnological and biomimetic applications [41, 50, 52, 98-100].  
201 Particularly, the repetitive physicochemical properties and isoporosity of S-layer protein lattices  
202 down to the sub-nanometer scale make them to unique matrices and building blocks for generating

203 complex, supramolecular assemblies. The prime attractiveness of such 'bottom-up' strategies lies in  
204 their capability to generate uniform nanostructures, and the possibility to exploit such structures at  
205 the meso- and macroscopic scale. Most importantly, it has been shown that S-layers can be combined  
206 with all major species of biological or synthesized (macro)molecules. Particularly, cloning and  
207 characterization of genes encoding S-layer proteins opened new areas of applied S-layer research as  
208 the incorporation of single or multifunctional domains is now possible without loss of their self-  
209 assembly capabilities [88]. As S-layers are highly anisotropic structures with regard to their  
210 topography and the physicochemical properties of their inner and outer surface, it was essential to  
211 ensure the recrystallization of S-layer (fusion) proteins in defined orientation on solid supports (e.g.,  
212 polymers, metals, semiconductors) and lipid membranes [71, 77]. Hence, the biomimetic approach to  
213 copy the physicochemical properties of the cell envelope structures might be among others a  
214 distinguished solution for the generation of supporting scaffolds for lipid membranes.

215 The recognition of biosensors started with the introduction of the first generation glucose  
216 oxidase (GOx) biosensor in 1962 [101], which is still the most widely used biosensor up to date [102-  
217 105]. Electrochemical biosensors, as exemplified by the glucose sensor, do not suffer the drawback of  
218 high sensor setup complexity and costs because of their close link to developments in low-cost  
219 production of microelectronic circuits and their easy interface with normal electronic read-out and  
220 processing. Other inherent advantages of electrochemical biosensors are their robustness, easy  
221 miniaturization, excellent detection limits also with small analyte volumes, and ability to be used in  
222 turbid biofluids with optically absorbing and fluorescing compounds [103, 106, 107].

223 Analysis of the mass distribution and permeability properties of isolated S-layer lattices of  
224 various *Bacillaceae* revealed that they function as isoporous molecular sieves with a pore size of 4  
225 nm to 5 nm in diameter, corresponding to a molecular mass cut-off in the range of 30 kDa to 40 kDa  
226 [108-112]. S-layer ultrafiltration membranes (SUMs) are produced by depositing S-layer-carrying cell  
227 wall fragments or S-layer self-assembly products on microfiltration membranes, crosslinking the S-  
228 layer protein under a certain pressure and finally reducing the Schiff bases [109, 112]. Beside enzymes  
229 (GOx, invertase, peroxidase, glucuronidase,  $\beta$ -glucosidase, naringinase), also ligands (protein A,  
230 streptavidin, folate) or mono- and polyclonal antibodies have been immobilized on the SUMs [108].

231 Since S-layers constitute an immobilization matrix of only several nanometers thickness, the  
232 fabrication of unsurpassed thin sensing layers with densely packed functional biomolecules, in  
233 particular enzymes is possible [113-116]. The first amperometric sensor based on an S-layer lattice  
234 comprised of an SUM with covalently bound GOx [117]. The retained activity of the immobilized  
235 GOx was approximately 40%. In order to function as working electrodes, a layer of gold or platinum  
236 covered the enzyme loaded SUMs. The biosensor yields high signals (150 nA mm<sup>-2</sup> mmol<sup>-1</sup> glucose),  
237 fast response times (10-30 sec), linearity range up to 12 mM glucose, stability under working  
238 conditions of more than 48 hours, and no loss of GOx activity after a storage period of 6 month. A  
239 further achievement with S-layer-based amperometric biosensors was the generation of a three-  
240 enzyme sensor for sucrose [118]. For this purpose, the enzymes invertase, mutarotase and GOx were  
241 immobilized on S-layer fragments isolated from *Clostridium thermohydrosulfuricum* L111-69 via  
242 aspartic acid as spacer molecules. After deposition of the modified S-layer fragments on  
243 microfiltration membranes, the surface of this multifunctional device was covered with gold by  
244 sputtering to function again as working electrode. Amperometric sucrose measurements based on  
245 the oxidation of hydrogen peroxide revealed a high signal level (1  $\mu$ A cm<sup>-2</sup> mmol<sup>-1</sup> sucrose), 5 min  
246 response time and a linear range up to 30 mM sucrose. In a further approach, a glucose sensor with  
247 an oxygen optode as transducer containing a ruthenium(II) complex, whose fluorescence is  
248 dynamically quenched by molecular oxygen was developed [119]. For fabrication of this fibre-optic  
249 biosensor the GOx was covalently immobilized as a monolayer on SUMs. The performance of the  
250 biosensor in terms of response time, linear range and stability was comparable to existing optodes.  
251 However, this system holds great potential for the development of micro-integrated optical biosensor  
252 due to its tiny size. A further improvement of this fibre-optic glucose sensor was to connect the GOx  
253 molecules in its tightest packing immobilized on the S-layer lattice with an optimum metallic contact,  
254 which must not disturb the protein structure [120]. Previously, platinum films were applied on

255 enzyme layers immobilized on S-layer protein by argon sputtering. However, this conventional  
256 method exhibits substantial limitations, e.g., a volume change of the S-layer/enzyme composite  
257 system when it is introduced into a conventional vacuum coating apparatus. This drawback was  
258 circumvented by pulse-laser-deposition method. The latter approach resulted in an enzyme activity  
259 of 70-80%, which constitutes a doubling of the activity compared to first amperometric sensor based  
260 on an S-layer lattice [114, 117, 120]. Hence, this example demonstrates that composite system  
261 consisting of the 2D-protein-layer/enzyme/metal arrangement can successfully serve as high efficient  
262 biosensors.

263 The continuous, stable, and accurate detection of glucose in blood is a challenging task because  
264 many blood components disturb the measurement. As S-layer lattices constitute highly hydrated,  
265 ultrathin biological antifouling materials [121], Picher et al. developed a lab-on-a-chip comprising of  
266 embedded amperometric sensors in four S-layer-coated micro-reactors, which can be addressed  
267 individually [56]. The S-layer had the function to provide an efficient antifouling coating, a highly-  
268 oriented immobilization matrix for the GOx and an effective molecular sieve. Moreover, the S-layer  
269 protein SbpA from *L. sphaericus* CCM 2177 readily formed monomolecular lattice structures at the  
270 various microchip surfaces (e.g., glass, polydimethylsiloxane, platinum and gold) within one hour.  
271 The microfluidic device operated in a feedback loop mechanism and was used to assess natural  
272 variations in blood glucose levels during hemodialysis and hence, to allow the individual adjustment  
273 of glucose. To ensure reliable and accurate detection of glucose in blood the lab-on-a-chip performed  
274 simultaneously blood glucose measurements, autocalibration routines, mediator-interferences  
275 detection, and background subtractions. The highly isoporous SbpA-coating eliminated unspecific  
276 adsorption events in the presence of human serum albumin, human plasma and freshly-drawn blood  
277 samples. Most important, the undisturbed diffusion of the mediator to the electrode surface enabled  
278 electrochemical measurements of glucose in concentrations between 0.5 mM to 50 mM [56]. Hence,  
279 this combination of biologically-derived nanostructured surfaces with micro-chip technology  
280 constitutes a powerful tool for multiplexed analysis of complex samples.

281 The bioreceptor in cholesterol biosensors is very commonly the cholesterol oxidase (ChOx). A  
282 simple and reliable method to prepare reproducible and stable ChOx monolayers was to spread the  
283 ChOx at the water-air interface. Mixed films comprising of ChOx and S-layer proteins showed a long-  
284 term stability at the air-water interphase [122]. In a further study, the mixed film was transferred onto  
285 the surface of screen-printed carbon electrodes by the Langmuir-Blodgett technique [123]. The  
286 modified electrode surface was characterized by AFM and cyclic voltammetry (CV). AFM indicated  
287 the presence of deposited layers, which resulted also in a reduction of the surface roughness of the  
288 electrodes. As demonstrated by CV, the presence of S-layer proteins in the ChOx Langmuir-Blodgett  
289 film increased the oxidation peak intensity and reduced the oxidation potential. Therefore, these  
290 results showed the feasibility of producing a cholesterol biosensor based on the immobilization of a  
291 mixed film comprising of ChOx and S-layer proteins on screen-printed carbon electrodes [123].

292 For the development of oxygen sensors an oxygen sensitive Pt(II) porphyrin dye was covalently  
293 bound to the S-layer matrix [124]. The oxygen concentration was measured by phase modulation  
294 fluorimetry. Setups comprising low cost optoelectronic components like light emitting diodes and  
295 silicon photodiodes were constructed. For both sensor setups (planar and fiber optic) variations in  
296 the oxygen concentrations resulted in distinct and reproducible changes in the luminescence lifetime  
297 and intensity. The luminescence quenching efficiency of these sensors was found to be 1.5–1.9  
298 (expressed as the ratio of signal under nitrogen and air) which compares well to other sensor systems  
299 using luminophores embedded in polymer matrices. These results demonstrated the application  
300 potential of S-layers as immobilization matrices in the development of biosensors [124]. The general  
301 principle for the construction of optical sensors by immobilization of various dyes, fluorophores  
302 and/or receptors on monomolecular S-layer protein coatings can be applied for sensing of manifold  
303 analytes.

304 In a recent study, a monomolecular S-layer lattice comprising of the S-layer protein SbpA  
305 conjugated with folate was recrystallized on a gold surface [39]. This biorecognition layer ensured  
306 the specific capture of human breast adenocarcinoma cells (MCF-7) via the recognition of folate

307 receptors, which are expressed on the surface of MCF-7. The fabricated acoustic and electrochemical  
308 sensors were able to distinguish between MCF-7 and human liver hepatocellular carcinoma (HepG2)  
309 cells as the latter do not express folate receptors. This biosensor offers several advantages including  
310 the small thickness of the SbpA lattice, which increases cells capturing efficiency. Moreover, there is  
311 no requirement to block the surface due to the antifouling properties of the S-layer lattice and no  
312 awareness of antibody immobilization as folate can be used as an alternative to the antibody for  
313 capturing target cells. Over all, evaluating of the developed biosensors by different techniques  
314 provides more information about the efficiency of the system. QCM-D measurements tracked the  
315 formation of SbpA-folate modified sensor and capturing of cancer cells efficiently in real-time and  
316 under controlled conditions. Although the QCM-D technique shows a limited detection range, it  
317 allows tracking the cell viability [39]. Hence, the cellular response to chemotherapeutic agents is  
318 worth to be investigated in further QCM-D studies. Indeed, electrochemical measurements confirm  
319 the selectivity and specificity of the developed biosensor and provide a simple, rapid, cost-effective  
320 and disposable analysis of cancer detection. Moreover, the development of efficient biosensors for  
321 accurate diagnosis helps to increase the cure and survival rates of patients with cancer and provides  
322 great promise for effective analysis with high selectivity and sensitivity.

323 The S-layer protein from *L. sphaericus* JG-A12 was bound on a gold surface in order to fabricate  
324 a uranyl ( $\text{UO}_2^{2+}$ ) biosensor. Immobilization occurred either by binding of the cysteine of the S-layer  
325 protein to a SAM, which presented maleimide groups or to a mixed SAM presenting biotin, which  
326 bound neutravidin and the latter subsequently the biotinylated S-layer protein [125]. The new  
327 biosensor responds to picomolar levels of aqueous uranyl ions within minutes. In comparison to  
328 traditional SAM-based biosensors, the porous bioconjugated layer showed higher stability, longer  
329 electrode life span and a denser protein layer. The biosensors responded specifically to  $\text{UO}_2^{2+}$ -ions  
330 with a detection limit of  $10^{-12}$  M and showed minor interference from  $\text{Ni}^{2+}$ ,  $\text{Cs}^+$ ,  $\text{Cd}^{2+}$  and  $\text{Co}^{2+}$ .  
331 Chemical modification of the phosphate and carboxyl groups of the S-layer protein prevented  $\text{UO}_2^{2+}$   
332 binding, indicating that both moieties are involved in the recognition to  $\text{UO}_2^{2+}$  [125]. In future, it might  
333 be possible that S-layer protein isolates from bacteria surviving in other metal polluted sites may  
334 provide the sensing components for the fabrication of further biosensors for the detection of other  
335 metal ion.

#### 336 4. Genetically engineered S-layers as components in biosensors

337 Their intrinsic self-assembly properties as well as their periodicity make S-layers to ideal  
338 building blocks for all kinds of detection systems like DNA-, protein-, allergy- or antibody-chips as  
339 well as label-free detection systems (for review see [15, 52, 126]).

340 The construction of S-layer-streptavidin fusion proteins carrying core-streptavidin either at the  
341 N-terminus or C-terminus allowed the generation of universal affinity matrices for the specific  
342 binding of biotinylated molecules like, e.g., proteins, allergens, antibodies, oligonucleotides, or  
343 nanoparticles [89, 127, 128]. Another application potential is in the development of label-free  
344 detection systems. The specific binding of functional molecules to the sensor chip functionalized with  
345 an oriented chimaeric S-layer can be measured directly by determining the change in mass on the  
346 chip. In addition, there is no need for any labeling if the applied transducer relies upon surface-  
347 sensitive techniques like QCM-D, SPR or SAW.

348 Proof-of-principle for label-free detection systems based on S-layer proteins was performed with  
349 the S-layer fusion protein incorporating the sequence of a variable domain of a heavy chain camel  
350 antibody directed against prostate-specific antigen (PSA) [129, 130]. After recrystallization of the S-  
351 layer fusion protein on gold chips, the monomolecular protein lattice was exploited as sensing layer  
352 in SPR biochips to detect PSA. A further application for this chimaeric S-layer fusion protein was to  
353 recrystallize them on silica microbeads. These S-layer fusion protein-covered microbeads were  
354 applied as biocompatible matrix at a microsphere-based detoxification system used for  
355 extracorporeal blood purification of patients suffering from autoimmune disease [131].

356 In another approach, the recombinant S-layer fusion protein rSbpA/ZZ incorporating two copies  
357 of the Fc-binding Z-domain, which is a synthetic analogue of the IgG-binding domain of protein A

358 from *Staphylococcus aureus* was constructed. Most important, the ZZ-domains remained exposed  
359 on the outermost surface of the S-layer fusion protein lattice. As determined by SPR measurements,  
360 the binding capacity of the self-assembled rSbpA/ZZ monolayer for human IgG was 5.1 ng/mm<sup>2</sup>,  
361 which corresponded to 78% of the theoretical saturation capacity of a planar surface for IgGs aligned  
362 in the upright position [132]. rSbpA/ZZ has also been recrystallized on the surface of cellulose-based  
363 microbeads. Compared to commercial particles used as immunoadsorbents to remove autoantibodies  
364 from sera of patients suffering from an autoimmune disease, the IgG binding capacity of the S-layer  
365 fusion protein-coated microbeads was at least 20 times higher [132]. Hence, this novel type of  
366 microbeads should find application in the microsphere-based detoxification system. Recently, an  
367 efficient acoustic and hybrid three-dimensional-printed electrochemical biosensors based on  
368 rSbpA/ZZ for the detection of liver cancer cells was developed [37]. The biosensors function by  
369 recognizing the highly expressed tumor marker CD133, which is located on the surface of liver cancer  
370 cells. Detection was achieved by recrystallizing rSbpA/ZZ on the surface of the sensors. The fused  
371 ZZ-domain enabled immobilization of the anti-CD133 antibody in a defined manner. These highly  
372 accessible anti-CD133 antibodies were employed as a sensing layer for the efficient detection of  
373 HepG2 cells. The recognition of HepG2 cells was investigated in situ using QCM-D and CV, which  
374 confirmed the efficiency of the fabricated sensors to perform label-free and real-time detection of  
375 living cells. Most importantly, these sensors offer low-cost and disposable detection platforms for  
376 real-world applications. Hence, both fabricated acoustic and electrochemical sensing platforms can  
377 detect cancer cells and therefore may have further potential in other clinical applications and drug-  
378 screening studies [37].

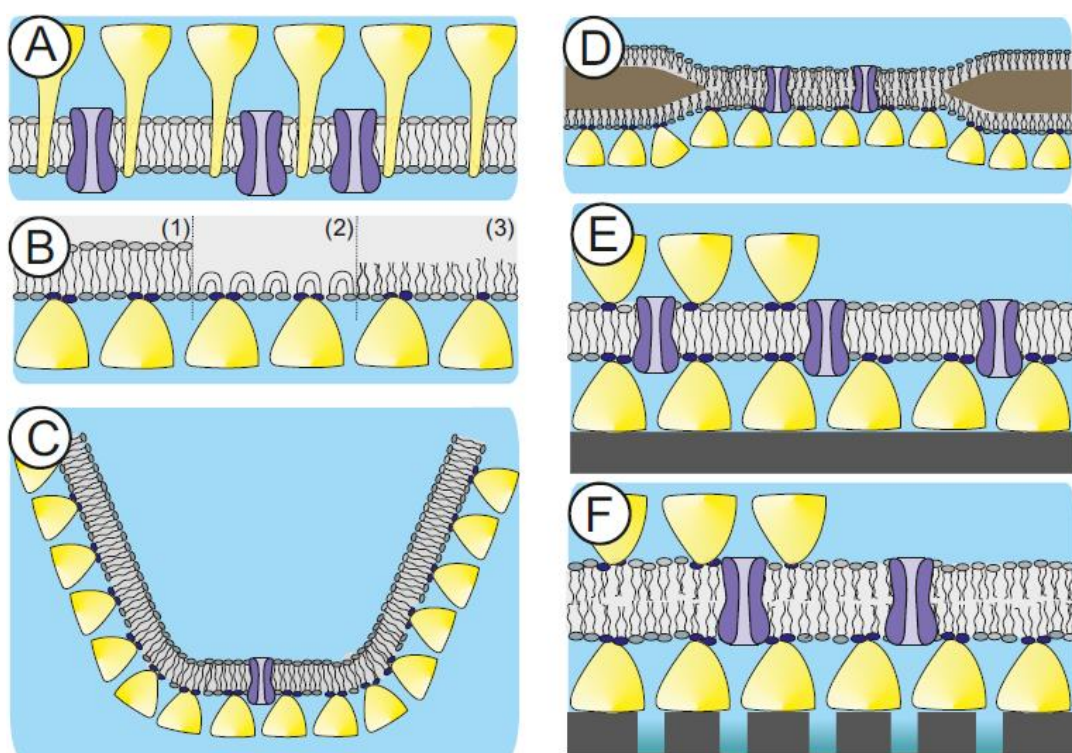
379 For another field of research S-layer fusion proteins comprising of SbpA or SbsB, the S-layer  
380 protein from *Geobacillus stearothermophilus* PV72/p2 and peptide mimotopes such as F1, that mimics  
381 an immunodominant epitope of Epstein–Barr virus (EBV) were constructed [133, 134]. Diagnostic  
382 studies have been performed by screening 83 individual EBV IgM-positive, EBV-negative, and  
383 potential cross-reactive sera and resulted in 98.2% specificity and 89.3% sensitivity as well as no cross-  
384 reactivity with related viral diseases. This result demonstrated the potential of these S-layer fusion  
385 proteins to act as a matrix for site-directed immobilization of small ligands in solid phase  
386 immunoassays.

387 Finally, the laccase of *Bacillus halodurans* C-125 was immobilized on the S-layer lattice formed by  
388 SbpA either by covalent linkage of the enzyme or by construction of a fusion protein comprising the  
389 S-layer protein and the laccase (rSbpA/Lac) [135]. The specific activity of the free, immobilized, and  
390 fused laccase was proven because all showed laccase-like activity oxidizing 2,2'-azino-bis(3-  
391 ethylbenzthiazoline-6-sulfonic acid), 2,6-dimethoxyphenol, syringaldazine, and hydroquinone.  
392 Interestingly, the S-layer part confers a much higher solubility on the laccase as observed for the sole  
393 enzyme. Comparative spectrophotometric measurements of the enzyme activity revealed similar but  
394 significantly higher values for laccase and rSbpA/Lac in solution compared to the immobilized state,  
395 respectively. However, laccase covalently linked to the SbpA monolayer yielded a four to five time  
396 higher enzymatic activity than rSbpA/Lac immobilized on a solid support. Combined QCM-D and  
397 electrochemical measurements revealed that the laccase immobilized on the SbpA lattice had an  
398 approximately twofold higher enzymatic activity compared to that obtained with rSbpA/Lac [135].

## 399 5. S-layer lattices for generation of functional lipid membrane platforms

400 The cell envelope structure of some archaeal species (e.g., *Sulfolobus* spp.) constitute simply of a  
401 cytoplasma membrane comprising of etherlipids and a membrane-anchored S-layer lattice (Figure 3  
402 A) [44, 136]. In a biomimetic approach, this supramolecular cell envelope structure constitutes the  
403 building plan for SsLMs (Figure 3 B-F). It is assumed that the cell envelope structure of archaea is a  
404 key prerequisite for these organisms to be able to dwell under extreme environmental conditions  
405 such as temperatures up to 120 °C, pH down to 0, high hydrostatic pressure, or high salt  
406 concentrations [42, 137, 138]. Hence, S-layer lattices may therefore be very important to provide basic  
407 functions like mechanical and osmotic cell stabilization [139, 140]. As suitable methods for  
408 disintegration of archaeal S-layer protein lattices and their reassembly into monomolecular arrays on

409 lipid films are not yet available, S-layer proteins from Gram-positive bacteria are used for the  
 410 generation of SsLMs [41, 93, 95, 97, 98, 141]. In addition, a second S-layer acting as protective  
 411 molecular sieve and further stabilizing scaffold and antifouling layer can be recrystallized on the top  
 412 of the previously generated SsLM (Figure 3 E, F). These features make S-layer lattices to unique  
 413 supporting architectures resulting in lipid membranes with nanopatterned fluidity and considerably  
 414 extended longevity [41, 93-95, 97, 98, 142-144].  
 415



416  
 417 Figure 3: Scheme of natural and S-layer supported lipid membranes. Supramolecular structure of an  
 418 archaeal cell envelope comprising of a cytoplasma membrane, archaeal S-layer proteins incorporated  
 419 in the lipidic matrix and integral membrane proteins (A). Schematic illustrations of various S-layer-  
 420 supported lipid membranes. (B) Lipid monolayer films at the air/water interphase with an  
 421 underneath recrystallized S-layer lattice. (1) Tetraether lipid monolayer in the upright conformation.  
 422 (2) Tetraether lipid monolayer in the U-shaped (bent) conformation. (3) Phospholipid monolayer. (C)  
 423 A tetraether lipid monolayer membrane is generated across an orifice of a patch clamp pipette by the  
 424 tip-dip method. Subsequently a closely attached S-layer lattice is formed by bacterial S-layer proteins  
 425 on one side of the lipid membrane. In (D), a folded or painted bilayer phospholipid membrane  
 426 spanning a Teflon aperture is shown. A closed bacterial S-layer lattice can be self-assembled on either  
 427 one or both (not shown) sides of the lipid membrane. (E) Schematic drawing of a solid support where  
 428 a closed bacterial S-layer lattice has been assembled. On this biomimetic structure a tetraether lipid  
 429 membrane was generated by the modified Langmuir-Blodgett method. Optionally as shown on the  
 430 left side, a bacterial S-layer lattice can be attached on the external side of the solid supported lipid  
 431 membrane. (F) Scheme of a bilayer lipid membrane generated on an S-layer ultrafiltration membrane.  
 432 Optionally as shown on the left side, a bacterial S-layer lattice can be attached on the external side of  
 433 the SUM-supported lipid membrane. In B to F, the head groups of the lipid molecules interacting  
 434 with the S-layer protein are marked in dark. As indicated in C to F, all S-layer-supported model lipid  
 435 membranes can be functionalized by biomolecules like membrane-active peptides and integral  
 436 membrane proteins. Modified after [63], copyright (2004) with permission from Wiley-VCH.  
 437

438 The interaction of the S-layer proteins SbpA and SbsB with lipid molecules has been investigated  
 439 in detail [78-80, 145]. It turned out that most probably negatively charged moieties on the S-layer  
 440 protein interact via electrostatic interaction with the head groups of zwitterionic and/or positively  
 441 charged lipids (Table 1). As natural, wild-type S-layer proteins possess frequently a so-called S-layer

442 homologous domain, which interact with the secondary cell wall polymer, the latter can be coupled  
443 to the head group of a lipid and the lipid can be immobilized via a lectin-type like binding on the S-  
444 layer protein [18]. The recrystallized S-layer protein can also be chemically modified in order to bind  
445 lipids with head groups comprising of a primary amine group [146, 147], thiol group [148], or  
446 maleimide group (Table 1). Moreover, a linker like, e.g., streptavidin can be coupled to the S-layer  
447 protein, which allows a strong ligation of biotinylated lipids [149, 150]. Finally, the S-layer protein  
448 can be genetically engineered so that either a thiol group from an introduced cysteine, multiple  
449 histidines (His-tag), streptavidin, or a strept-tag is exposed on the S-layer lattice (Table 1). These  
450 modifications allow the coupling of lipids carrying a maleimide group [151-153], nickel(II)-  
451 nitrilotriacetic acid anchor [154], or biotin at their head group region [73, 155, 156], respectively.

452 In general, S-layer proteins can be recrystallized on either a lipid monolayer generated at the air-  
453 water interface (Figure 3 B), a preformed lipid membrane like a planar, freestanding lipid bilayer  
454 (Figure 3 C, D) or a spherical liposome or emulsome (Figure 4). Moreover, the lipid membrane can  
455 be generated on an already existing recrystallized S-layer lattice (Figure 3 E, F). The latter approach  
456 is the method of choice to generate functional lipid membrane platforms, which are, beside other  
457 applications, a straightforward approach in the development of biosensors [41, 144].

458 SsLMs prepared by the Langmuir-Blodgett/Langmuir-Schaefer technique without the need on  
459 an aperture has been compared to silane- and dextran-supported phospholipid bilayer [157]. Most  
460 probably due to the repetitive local interaction of the S-layer lattice with the lipid head groups, the  
461 nanopatterned fluidity of lipids was highest in SsLMs compared to the other supported bilayers as  
462 determined by the fluorescence recovery after photobleaching technique. Phospholipid bilayers and  
463 tetraether lipid monolayers have also been generated on S-layer covered gold electrodes. The  
464 tetraether lipid monolayer sandwiched by an S-layer lattice on each side (Figure 3 E) revealed an  
465 exceptional long-term robustness of approximately one week [41, 93, 96-98]. This finding reflects also  
466 the optimization of the archaeal cell envelope structure by Nature over billions of years of evolution.

467 Lipid membranes generated on a porous support combine the advantage of easy manual  
468 handling, individual excess to both membrane surfaces, and possessing an essentially unlimited ionic  
469 reservoir on each side of the bilayer lipid membrane (BLM; Figure 3 F). This is seen as basic  
470 requirement of experiments copying the *in vivo* situation (e.g., plasmatic / exoplasmatic side).  
471 However, the surface properties of porous supports, like roughness or great differences in pore size  
472 have significantly impaired the stability of attached BLMs [158]. Hence, a straightforward approach  
473 is the use of SUMs with the S-layer as stabilizing and smoothening layer between the lipid membrane  
474 and the porous support [159-161].

475 SUMs were produced by depositing S-layer fragments as a coherent layer on microfiltration  
476 membranes [109, 111, 162]. The mechanical and chemical stability of their composite structure is  
477 subsequently obtained by inter- and intramolecular cross-linking [109, 110, 162-164]. The uniformity  
478 of functional groups on both, the surface and within the pore area of the S-layer lattice could be used  
479 for very accurate chemical modifications in the sub-nanometer range allowing to tune the molecular  
480 sieving as well as antifouling characteristics of SUMs [162, 163, 165]. Moreover, SUMs can be  
481 prepared with different net charges and hydrophilic or hydrophobic surface properties. That is why  
482 SUMs have been used as supporting and stabilizing structures for functional lipid membranes [15,  
483 41, 94, 97, 144].

484 Whereas composite SUM-supported phospholipid bilayers were found to be highly isolating  
485 structures with a life-time of up to 17 hours [159-161], BLMs on plain microfiltration membranes  
486 revealed only a life-time of approximately 3 hours. The life time increased significantly to about one  
487 day by formation of an S-layer – lipid membrane – S-layer sandwich-like structure, i.e. an additional  
488 monomolecular S-layer protein lattice recrystallized on the lipid-faced side (Figure 3 F) [159, 160]. An  
489 even further increase in the stability of this composite supramolecular structure can be expected upon  
490 crosslinking of those lipid head groups, which are directly in contact with domains on the S-layer  
491 protein. Hence, the nanopatterned anchoring of the membrane is a promising strategy for generating  
492 stable and fluid lipid membranes [86].

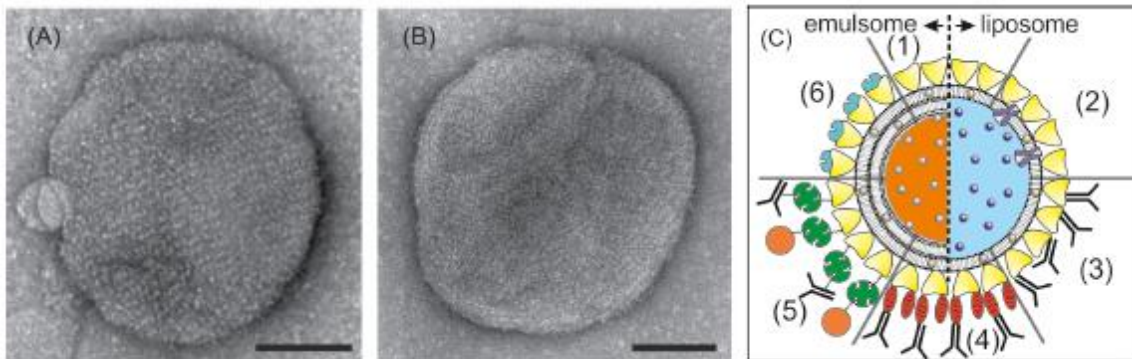
493

494 Table 1: Immobilization strategies. Summary of the to date investigated strategies to bind lipid  
 495 molecules on S-layer protein lattices (modified after [41]).

Type	Reactive group	Crosslinker	Targeted group	References
<b>Natural SPLs</b>				
Electrostatic interaction	Negatively charged groups on SLP		Zwitterionic or positively charged lipids	[79, 80, 145]
Lectin-type like binding	S-layer homologous domain on SLP		Secondary cell wall polymer coupled to lipids	[18]
<b>Chemical modification of SPLs</b>				
Covalent bond	Carboxyl groups on SLP	Carbodiimide analogues	Primary amine group from lipids	[146, 147, 168]
Covalent bond	Primary amino groups on SLP	SMCC analogues	Thiol group from lipids	[148]
Covalent bond	Primary amino groups on SLP	SPDP/TCEP; insertion of thiol group in SLP	Maleimide group from lipids	Schuster et al., in preparation
<b>Chemical binding of linker on SPLs</b>				
Strong ligation	Streptavidin chemically coupled to SLP		Biotinylated lipids	[149, 150]
<b>Genetically engineered SPLs</b>				
Covalent bond	Thiol-group from introduced cysteine		Maleimide group from lipids	[151-153]
Multiple chelation	Multiple histidines (His6-tag) on SLP		Nickel(II)-NTA from lipids	[154]
Strong ligation	Streptavidin fused to SLP		Biotinylated lipids	[89]
Strong ligation	Strep-tag fused to SLP	Streptavidin	Biotinylated lipids	[72, 73, 155]

SLP: S-layer protein; SMCC: Succinimidyl-4-(*N*-maleimidomethyl)cyclohexane-1-carboxylate; SPDP: *N*-Succinimidyl 3-(2-pyridyldithio)-propionate; TCEP: Tris (2-carboxyethyl) phosphine hydrochloride; NTA: nitrilotriacetic acid.

496 The functionality of SsLMs resting on solid supports has been investigated by the incorporation  
 497 of the membrane-active peptides valinomycin, alamethicin, gramicidin D, and the antimicrobial  
 498 peptide analogue PGLa(-) (Table 2) [159, 166, 167]. SsLMs with incorporated valinomycin, a  
 499 potassium-selective ion carrier, revealed a remarkable high resistance bathed in sodium buffer.  
 500 However, bathed in potassium buffer a decrease in resistance by a factor of 500 is observed for the  
 501 same membrane due to the valinomycin-mediated potassium transport [159].



502  
 503 Figure 4: S-layer-coated liposomes and emulsomes. TEM images of emulsomes coated with the S-  
 504 layer protein SbsB from *Geobacillus stearothermophilus* PV72/p2 (A) wildtype SbsB and (B)  
 505 recombinant SbsB. The bars correspond to 100 nm. Adopted from [191], copyright (2013) with  
 506 permission from Wiley–VCH. (C) Schematic drawing of (1) an S-layer coated emulsomes (left) and  
 507 liposome (right) with entrapped functional molecules and (2) functionalized by reconstituted integral  
 508 proteins. Note, S-layer coated emulsomes and liposomes can be used as immobilization  
 509 matrix for functional molecules (e.g., human IgG) either by direct binding (3) or by immobilization  
 510 via the Fc-specific ligand protein A (4), or biotinylated ligands can be bound to the S-layer coated  
 511 liposome or emulsomes via the biotin – avidin system (5). Alternatively, emulsomes or liposomes can  
 512 be coated with genetically modified S-layer subunits incorporating functional domains (6). Modified  
 513 after [61], copyright (2002) with permission from Wiley–VCH.  
 514  
 515

516 Table 2: Membrane-active peptides. Summary of membrane-active peptides incorporated in S-layer  
 517 supported lipid membranes (modified after [41]).

Membrane-active peptide	Source	Remarks	References
gramicidin A (gA)	<i>Bacillus brevis</i>	linear pentadeca peptide	[161]
alamethicin (Ala)	<i>Trichoderma viride</i>	linear, 20 amino acids	[159]
valinomycin (Val)	several <i>Streptomyces</i> strains, e.g., <i>S. tsusimaensis</i> and <i>S. fulvissimus</i>	cyclic dodecadipeptide, 12 amino acids and esters	[141, 159]
peptidyl-glycine-leucine-carboxyamide (PGLa) analogue	synthesized via protein chemistry	20 amino acid; negatively charged analogue of PGLa	[168]

518  
 519 SsLMs generated by the rapid solvent exchange technique were utilized to perform combined  
 520 surface-sensitive QCM-D and EIS measurements. This study evidenced not only the attachment  
 521 and/or insertion of PGLa(-) in the supported lipid membrane but also indicated toroidal pore  
 522 formation in a concentration dependent fashion [168]. Hence, SsLMs constitute a promising platform  
 523 for studying the interaction and insertion of membrane-active (antimicrobial) peptides [169, 170].

524 Incorporation of the membrane-active peptide gramicidin D could be demonstrated by  
 525 measurements on single gramicidin D pores in all above mentioned SsLMs [161].

526 Finally, alamethicin channels could not only be incorporated in SsLMs on solid supports, the  
 527 channels could even be specifically blocked as increasing amounts of inhibitor (amiloride) gave rise  
 528 to a significant increase in membrane resistance (Table 2) [159]. Thus, proof of concept for the  
 529 applicability of these composite S-layer/lipid structures for biosensing purposes has been  
 530 demonstrated. In future, the ability to reconstitute integral membrane proteins in defined structures

531 on, e.g., sensor surfaces is one of the most important concerns in designing biomimetic sensing  
 532 devices [41, 171-173].

533 Membrane proteins have also been successfully reconstituted in SsLMs (Table 3). Reconstitution  
 534 of  $\alpha$ -hemolysin ( $\alpha$ HL), moreover even single pore recordings could be achieved with SUM-supported  
 535 phospholipid bilayers but no pore formation was observed with BLMs generated on the pure micro  
 536 filtration membranes [160].

537

538 Table 3: Transmembrane proteins. Summary of transmembrane proteins reconstituted in S-layer  
 539 supported lipid membranes (modified after [41]).

Transmembrane protein	Source	Remarks	References
$\alpha$ -hemolysin ( $\alpha$ HL)	exotoxin from <i>Staphylococcus aureus</i>	pore-forming; homo-heptamer	[144, 160]
ryanodine receptor 1 (RyR1)	skeletal muscle cells	$\text{Ca}^{2+}$ -release channel; homotetramer	[174]
nicotinic acetylcholine receptor (nAChR)	plasma membranes of neurons; on post-synaptic side of the neuromuscular junction	ligand gated ion channel; 5 subunits	[154]
voltage-dependent anion channel (VDAC)	located on the outer mitochondrial membrane; also produced by cell-free expression	porin, voltage gated; ion channel monomeric but can cluster	[175]

540

541 The ryanodine receptor, RyR1, isolated from rabbit muscle cells was successfully reconstituted  
 542 in SsLMs [174]. For this purpose, SsLMs were formed by the  $\beta$ -diketone ligand europium-triggered  
 543 vesicle fusion technique [147] either on glass (for fluorescence experiments) or on gold (for QCM-D  
 544 measurements). Preliminary measurements clearly indicated that incorporation of RyR1 occurred,  
 545 which was verified by control experiments to exclude misinterpretation due to unspecific adsorption  
 546 of RyR1 to the bilayer or the S-layer lattice [174]. Nevertheless, further experiments like, e.g.,  
 547 combined QCM-D with EIS studies or patch clamp measurements on a chip have to be performed.  
 548 Finally, SsLMs may constitute versatile and stabilizing scaffold allowing the detailed investigation of  
 549 different drugs on isolated RyR1 in high-throughput screening like devices.

550 SsLMs made by the newly developed the  $\beta$ -diketone ligand europium-triggered vesicle fusion  
 551 technique [147] were incubated with the voltage-dependent anion channel (VDAC; Table 3). A  
 552 significant decrease in membrane resistance could be observed but the membrane capacitance did  
 553 not change significantly. Moreover, increasing VDAC concentration decreased the membrane  
 554 resistance, which indicated increasing number of channels reconstituted spontaneously into the  
 555 SsLM [175]. It is well known that VDAC reconstituted in artificial membranes forms a voltage-gated  
 556 channel. At low membrane potentials (less than 10 mV) VDAC is in the open state and switches to the  
 557 closed state at high membrane potentials [176-178]. Indeed, this behaviour could also be clearly  
 558 observed for the SsLMs with incorporated VDAC channels. Furthermore, the membrane resistance  
 559 decreased again after reducing the voltage from 10 mV back to zero but the resistance was higher  
 560 compared to the first measurement. This may be explained by the re-opening of some channels while  
 561 others remain closed. In addition, it is conceivable that keeping the channels in the closed state for a  
 562 long period during the measurements may reduce the rate of re-opening of VDAC and cause some  
 563 structural rearrangements in order to achieve a more stable closed conformation [177, 179]. Moreover,  
 564 it has been shown that the presence of the nucleotides nicotinamide adenine dinucleotide hydride  
 565 (NADH) or nicotinamide adenine dinucleotide phosphate hydrogen induce channel closure and  
 566 thus, the conductance of the VDAC channels is significantly reduced [180-183]. Indeed, addition of

567 NADH to the SsLM with reconstituted VDAC caused a significant increase of the membrane  
568 resistance, which is a strong evidence for the blocking of VDAC channels by NADH molecules [175].

569 All the before mentioned examples for the functional reconstitution of membrane-active  
570 peptides and membrane proteins in SsLMs are currently proof-of-principle studies. However, there  
571 is a strong desire to use them in particular to probe function of membrane proteins, e.g., in drug  
572 screening applications. In this context it is interesting to note, that membrane proteins currently  
573 comprise more than 50% of all drug targets and many of these proteins are directly involved in charge  
574 transfer processes across the membrane [184, 185]. A direct electrical readout of ionic currents  
575 generated by ion channels, for example, bears the advantage of an amplification of the readout signal  
576 of membrane functions without need for labelling compared to current state-of-the-art techniques for  
577 membrane protein screening.

578 Vesicular lipid structures like unilamellar liposomes, comprising of a closed, spherical lipid  
579 mono- or bilayer with an aqueous inner space and emulsomes, comprising of a solid fat core  
580 surrounded by lipid layers are mainly used as drug targeting and drug delivery systems [186, 187].  
581 However, these lipid nanoparticles can also be used as biosensors for diagnosis purposes if the drug  
582 is replaced or supplemented by a radiotracer, contrast agent or a fluorescent dye. The use of  
583 molecular imaging to measure non-invasively the *in vivo* distribution of nanomedicines becomes  
584 increasingly important [188]. Labeling the nanoparticle gives also an indication of delivery to the  
585 target tissue. In this context, it is worth to mention that liposomes and emulsomes can be covered by  
586 an S-layer lattice (Figure 4 A, B) [150, 189-192]. In addition, the S-layer lattice may be functionalized  
587 with, e.g., antibodies in order to detect cancer cells (Figure 4 C). Moreover, S-layer-coated and with  
588 labelling agents loaded liposomes or emulsomes may be used for molecular imaging to detect, e.g.,  
589 inflammations in a body.

## 590 6. Conclusions & Outlook

591 One of the most challenging progress created by the development and research at the  
592 intersection of biological and engineering sciences are biosensors, which are becoming one of the  
593 most popular scientific areas. Significant progress in issues like miniaturization, functional  
594 sensitivity, simplified read-out, multiplexing, and utilization of newly discovered physical  
595 phenomena pushed further the development of smart devices. Moreover, semiconducting  
596 technology has proceeded in a way that in the field of biosensors a rapid infiltration of new  
597 (bio)nanotechnology-based approaches occurred. Due to bottom-up self-assembly processes at the  
598 nanometer scale, the traditional separation between transducers and bioreceptors is not valid any  
599 more. Indeed, by an integrative approach, the interface architecture take part in the recognition event  
600 and the receptors become active transducing elements of the biosensors (Figure 1).

601 The present Feature Paper describes the successful implementation of cell envelope components  
602 like, e.g., phospho- and etherlipids and in particular bacterial S-layer proteins in biosensors. S-layer  
603 proteins can be self-assembled to become part of the interface architecture and thereby connecting  
604 the bioreceptor to the transducer interface. The recrystallized S-layer lattice provide significant  
605 advantages over other coatings, which can be summarized as following: 1) S-layers are very thin  
606 structures (5 nm to 10 nm). This becomes very important if one uses surface-sensitive phenomena as  
607 transducer as it is indicated in Fig. 1. Because these techniques have a limited measuring range, the  
608 sensitivity decreases with increasing intermediate layer thickness. 2) S-layers are highly porous  
609 structures (30% to 70% porosity). This becomes very important if one uses electrochemical methods  
610 as transducer. Due to the electrolyte-filled pores, there is much less limitation of ions and the S-layer  
611 lattice itself shows a negligible resistance and capacitance. 3) The S-layer lattice presents functional  
612 groups in a well-defined special distribution and orientation. This property allows to bind  
613 bioreceptors densely packed and highly directed on the interface. 4) The S-layer lattice shows an anti-  
614 fouling, self-cleaning surface where almost no biomolecules stick to it. This characteristic is  
615 favourably when the measured signal corresponds to the bound and adsorbed biomolecules on the  
616 sensor surface. Finally, 5) the S-layer lattice can completely cover areas in the cm<sup>2</sup>-range by a one-  
617 step process. Hence, a coherent proteinaceous coating can functionalize the whole surface of

618 commonly used transducers. Although only little material is necessary, a possible drawback of using  
619 S-layer proteins is the need for the scale-up of the cultivation of bacteria and the isolation, subsequent  
620 purification and storage of S-layer proteins. However, recombinant production of S-layer proteins  
621 may help to overcome this issue. Moreover, physicists have to consider adopting certain protocols to  
622 meet the demands of biological materials.

623 As previously mentioned, S-layer lattices are because of their structural features highly suitable  
624 to immobilize biosensor-relevant molecules like enzymes, dyes, fluorophores and receptors. In  
625 another approach, the bioreceptor may be fused to the S-layer protein. The S-layer protein  
626 recrystallizing part ensures a layer presenting the bioreceptor molecules like enzymes, antibodies,  
627 IgG-binding domains and peptide mimotopes in a tight packing and rectified orientation. The S-layer  
628 lattice is used also as an anchoring scaffolding and/or ion reservoir in the generation of lipid  
629 membrane platforms. In contrast to tethered lipid membranes, where a precisely balanced mixture  
630 of tether and spacer molecules have to be assembled on the sensor surface, only one type of  
631 biomolecules, the S-layer protein is sufficient to provide few repetitive anchoring points for the lipid  
632 membrane.

633 Moreover, biologically inspired lipid membrane-based platforms enabled unprecedented signal  
634 amplification down to single-molecule sensitivity. This was achieved by the creation of mechanically  
635 and chemically stable membrane platforms with a high longevity. A further crucial property of  
636 membrane platforms is their ability to host membrane-associated and -integrated biomolecules like  
637 membrane-active peptides, ionophores, pore-forming proteins, ion channels or (G-protein coupled)  
638 receptors in a functional form. All these, in many cases highly sensitive biomolecules distinguish  
639 themselves by operating at very low concentrations of, e.g., ligands. For instance, ion channels and  
640 G-protein coupled receptors are highly sophisticated nanomachines that successfully solve the  
641 problem of selective and efficient amplification of a binding event.

642 Membrane platforms can be miniaturized in a chip format and allow very sensitive recording of  
643 single protein activity by, e.g., voltage-clamp electrochemical setups. Such systems are promising for  
644 drug discovery since they directly measure membrane protein functionality when they are exposed,  
645 e.g., to drug candidates. At present, biosensor research is not only driving the ever-accelerating race  
646 to construct smaller, faster, cheaper and more efficient devices, but may also ultimately result in the  
647 successful integration of electronic and biological systems. Any advancement in this field will have  
648 an effect on the future of diagnostics and health care. Personalized and preventive medicine, bedside  
649 diagnostics, and drug discovery will all benefit from the novel electronic sensing technologies.  
650

651 **Acknowledgments:** The financial support provided by the Austrian Science Fund (FWF), project P 29399-B22 is  
652 gratefully acknowledged.

653

654 **Conflicts of Interest:** The author declares no conflict of interest.

655

## 656 Abbreviations

657	2D	two-dimensional
658	$\alpha$ HL	$\alpha$ -hemolysin
659	AFM	atomic force microscopy
660	BLM	bilayer lipid membrane
661	CD133	tumor marker
662	ChOx	cholesterol oxidase
663	CV	cyclovoltammetry
664	EBV	Epstein-Barr virus
665	EIS	electrochemical impedance spectroscopy
666	GOx	glucose oxidase
667	HepG2	human liver carcinoma cells

668	IgG	immunoglobulin G
669	MCF-7	human breast adenocarcinoma cell
670	nAChR	nicotinic acetylcholine receptor
671	NADH	nicotinamide adenine dinucleotide hydride
672	PGLa(-)	negatively charged analogue of peptidyl-glycylleucine-carboxyamide
673	PSA	prostate-specific antigen
674	QCM-D	quartz crystal microbalance with dissipation monitoring
675	RyR1	ryanodine receptor/Ca <sup>2+</sup> release channel
676	rSbpA/Lac	recombinant fusion protein comprising of SbpA and laccase
677	rSbpA/ZZ	recombinant fusion protein comprising of SbpA and two copies of the Fc-binding Z-domain (a synthetic analogue of the IgG-binding domain of protein A from <i>Staphylococcus aureus</i> )
680	SAM	self-assembled monolayer
681	SAW	surface acoustic waves
682	SbpA	S-layer protein of <i>Lysinibacillus sphaericus</i> CCM 2177
683	SbsB	S-layer protein of <i>Geobacillus stearothermophilus</i> PV72/p2
684	S-layer	two dimensional arrays of proteinaceous subunits forming surface layers on prokaryotic cells
686	SPR	surface plasmon resonance
687	SsLM	S-layer supported lipid membrane
688	SUM	S-layer ultrafiltration membrane
689	TEM	transmission electron microscopy
690	TIRFM	total internal reflection fluorescence microscopy
691	VDAC	voltage-dependent anion channel

692 **References**

693 1. Thévenot, D. R.; Toth, K.; Durst, R. A.; Wilson, G. S., Electrochemical biosensors: Recommended  
694 definitions and classification. *Biosens Bioelectron* **2001**, *16*, (1-2), 121-131.

695 2. Dugas, V.; Elaissari, A.; Chevalier, Y., Surface sensitization techniques and recognition receptors  
696 immobilization on biosensors and microarrays. In *Recognition Receptors in Biosensors*, 2010; pp 47-134.

697 3. Turner, A. P. F., Biosensors: Fundamentals and applications - Historic book now open access. *Biosens*  
698 *Bioelectron* **2015**, *65*, A1.

699 4. Cavalcanti, A.; Shirinzadeh, B.; Zhang, M.; Kretly, L. C., Nanorobot hardware architecture for medical  
700 defense. *Sensors* **2008**, *8*, (5), 2932-2958.

701 5. Schmidt, J. J.; Montemagno, C. D., Bionanomechanical systems. *Annu Rev Mater Res*, **2004**, *34*, 315-337.

702 6. Sackmann, E., Supported membranes: Scientific and practical applications. *Science* **1996**, *271*, (5245),  
703 43-48.

704 7. Rädler, J.; Sackmann, E., Functionalization of solids by ultrathin soft polymer films and polymer/lipid  
705 film composites: Modeling of cell surfaces and cell recognition processes. *Curr Opin Solid St M* **1997**, *2*,  
706 (3), 330-336.

707 8. Dubey, M.; Weidner, T.; Gamble, L. J.; Castner, D. G., Structure and order of phosphonic acid-based  
708 self-assembled monolayers on Si(100). *Langmuir* **2010**, *26*, (18), 14747-14754.

709 9. Lessel, M.; Bäumchen, O.; Klos, M.; Hähl, H.; Fetzer, R.; Paulus, M.; Seemann, R.; Jacobs, K., Self-  
710 assembled silane monolayers: An efficient step-by-step recipe for high-quality, low energy surfaces.  
711 *Surf Interface Anal* **2015**, *47*, (5), 557-564.

712 10. Lvov, Y.; Decher, G.; Möhwald, H., Assembly, structural characterization, and thermal behavior of  
713 layer-by-layer deposited ultrathin films of poly(vinyl sulfate) and poly(allylamine). *Langmuir* **1993**, *9*,  
714 (2), 481-486.

715 11. Vericat, C.; Vela, M. E.; Benitez, G.; Carro, P.; Salvarezza, R. C., Self-assembled monolayers of thiols  
716 and dithiols on gold: New challenges for a well-known system. *Chem Soc Rev* **2010**, *39*, (5), 1805-1834.

717 12. Sleytr, U. B.; Bayley, H.; Sara, M.; Breitwieser, A.; Küpcü, S.; Mader, C.; Weigert, S.; Unger, F. M.;  
718 Messner, P.; Jahn-Schmid, B.; Schuster, B.; Pum, D.; Douglas, K.; Clark, N. A.; Moore, J. T.;  
719 Winningham, T. A.; Levy, S.; Frithsen, I.; Pankovc, J.; Beale, P.; Gillis, H. P.; Choutov, D. A.; Martin, K.  
720 P., VI. Applications of S-layers. *FEMS Microbiol Rev* **1997**, *20*, (1-2), 151-175.

721 13. Sleytr, U. B.; Egelseer, E. M.; Ilk, N.; Messner, P.; Schäffer, C.; Pum, D.; Schuster, B., Prokaryotic cell  
722 wall components: Structure and biochemistry nanobiotechnological applications of S-layers. In  
723 *Prokaryotic Cell Wall Compounds: Structure and Biochemistry*, Springer Berlin Heidelberg: 2010; pp 459-  
724 481.

725 14. Sleytr, U. B.; Egelseer, E. M.; Ilk, N.; Pum, D.; Schuster, B., S-Layers as a basic building block in a  
726 molecular construction kit. *FEBS J* **2007**, *274*, (2), 323-334.

727 15. Sleytr, U. B.; Schuster, B.; Egelseer, E. M.; Pum, D., S-layers: Principles and applications. *FEMS*  
728 *Microbiol Rev* **2014**, *38*, (5), 823-864.

729 16. Sleytr, U. B.; Schuster, B.; Egelseer, E. M.; Pum, D.; Horejs, C. M.; Tscheliessnig, R.; Ilk, N.,  
730 Nanobiotechnology with S-layer proteins as building blocks. *Prog in Mol Biol and Transl*, **2011**, *103*,  
731 277-352.

732 17. Heibel, C.; Ruehe, J.; Knoll, W. In *Tethered membranes on solid supports*, American Chemical Society,  
733 Polymer Preprints, Division of Polymer Chemistry, 1997; pp 956-957.

734 18. Knoll, W.; Naumann, R.; Friedrich, M.; Robertson, J. W. F.; Lösche, M.; Heinrich, F.; McGillivray, D. J.;  
735 Schuster, B.; Gufler, P. C.; Pum, D.; Sleytr, U. B., Solid supported lipid membranes: New concepts for  
736 the biomimetic functionalization of solid surfaces. *Biointerphases* **2008**, 3, (2), FA125-FA135.

737 19. Sinner, E. K.; Ritz, S.; Naumann, R.; Schiller, S.; Knoll, W., Self-assembled tethered bimolecular lipid  
738 membranes. *Adv Clin Chem* **2009**, 49, 159-179.

739 20. Knoll, W.; Köper, I.; Naumann, R.; Sinner, E. K., Tethered bimolecular lipid membranes-A novel  
740 model membrane platform. *Electrochim Acta* **2008**, 53, (23), 6680-6689.

741 21. Sinner, E. K.; Knoll, W., Functional tethered membranes. *Curr Opin Chem Biol* **2001**, 5, (6), 705-711.

742 22. Jackman, J. A.; Knoll, W.; Cho, N. J., Biotechnology applications of tethered lipid bilayer membranes.  
743 *Materials* **2012**, 5, (12), 2637-2657.

744 23. Schiller, S. M.; Naumann, R.; Lovejoy, K.; Kunz, H.; Knoll, W., Archaea analogue thiolipids for  
745 tethered bilayer lipid membranes on ultrasmooth gold surfaces. *Angew Chem Int Ed* **2003**, 42, (2), 208-  
746 211.

747 24. Schiller, S. M.; Reisinger-Friebis, A.; Götz, H.; Hawker, C. J.; Frank, C. W.; Naumann, R.; Knoll, W.,  
748 Biomimetic lipoglycopolymers membranes: Photochemical surface attachment of supramolecular  
749 architectures with defined orientation. *Angew Chem Int Ed* **2009**, 48, (37), 6896-6899.

750 25. Grieshaber, D.; MacKenzie, R.; Vörös, J.; Reimhult, E., Electrochemical biosensors - Sensor principles  
751 and architectures. *Sensors* **2008**, 8, (3), 1400-1458.

752 26. Cooper, C. L.; Dubin, P. L.; Kayitmazer, A. B.; Turksen, S., Polyelectrolyte-protein complexes. *Current  
753 Opin Colloid In* **2005**, 10, (1-2), 52-78.

754 27. Halai, R.; Cooper, M., Label-free technologies: Which technique to use and what to watch out for! In  
755 *Methods in Pharmacology and Toxicology*, 2015; Vol. 53, pp 3-15.

756 28. Hoa, X. D.; Kirk, A. G.; Tabrizian, M., Towards integrated and sensitive surface plasmon resonance  
757 biosensors: A review of recent progress. *Biosens Bioelectron* **2007**, 23, (2), 151-160.

758 29. Chen, Q.; Tang, W.; Wang, D.; Wu, X.; Li, N.; Liu, F., Amplified QCM-D biosensor for protein based  
759 on aptamer-functionalized gold nanoparticles. *Biosens Bioelectron* **2010**, 26, (2), 575-579.

760 30. Poitras, C.; Tufenkji, N., A QCM-D-based biosensor for E. coli O157:H7 highlighting the relevance of  
761 the dissipation slope as a transduction signal. *Biosens Bioelectron* **2009**, 24, (7), 2137-2142.

762 31. Tang, W.; Wang, D.; Xu, Y.; Li, N.; Liu, F., A self-assembled DNA nanostructure-amplified quartz  
763 crystal microbalance with dissipation biosensing platform for nucleic acids. *Chem Commun* **2012**, 48,  
764 (53), 6678-6680.

765 32. Yakovleva, M. E.; Safina, G. R.; Danielsson, B., A study of glycoprotein-lectin interactions using  
766 quartz crystal microbalance. *Anal Chim Acta* **2010**, 668, (1), 80-85.

767 33. Chang, B. Y.; Park, S. M., Electrochemical impedance spectroscopy. In *Annu Rev Anal Chem* **2010**, 3,  
768 207-229.

769 34. Daniels, J. S.; Pourmand, N., Label-free impedance biosensors: Opportunities and challenges.  
770 *Electroanalysis* **2007**, 19, (12), 1239-1257.

771 35. Kang, X.; Wang, J.; Wu, H.; Aksay, I. A.; Liu, J.; Lin, Y., Glucose Oxidase-graphene-chitosan modified  
772 electrode for direct electrochemistry and glucose sensing. *Biosens Bioelectron* **2009**, 25, (4), 901-905.

773 36. Katz, E.; Willner, I., Probing biomolecular interactions at conductive and semiconductive surfaces by  
774 impedance spectroscopy: Routes to impedimetric immunosensors, DNA-sensors, and enzyme  
775 biosensors. *Electroanalysis* **2003**, 15, (11), 913-947.

776 37. Damiati, S.; Küpcü, S.; Peacock, M.; Eilenberger, C.; Zamzami, M.; Qadri, I.; Choudhry, H.; Sleytr, U.  
777 B.; Schuster, B., Acoustic and hybrid 3D-printed electrochemical biosensors for the real-time  
778 immunodetection of liver cancer cells (HepG2). *Biosens Bioelectron* **2017**, *94*, 500-506.

779 38. Damiati, S.; Peacock; Leonhardt, S.; Damiati, L.; Baghdadi, M.; Becker, H.; Kodzius, R.; Schuster, B.,  
780 Embedded Disposable Functionalized Electrochemical Biosensor with a 3D-Printed Flow Cell for  
781 Detection of Hepatic Oval Cells (HOCs). *Genes* **2018**, *9*, 89.

782 39. Damiati, S.; Peacock, M.; Sleytr, U.; Schuster, B., Bioinspired Diagnostic Sensor Based on Functional  
783 Nanostructures of S-Proteins to Target the Folate Receptors in Breast Cancer Cells. *Sensor Actuat B-  
784 Chem* **2018**, submitted.

785 40. Sapsford, K. E.; Ligler, F. S., Real-time analysis of protein adsorption to a variety of thin films. *Biosens  
786 Bioelectron* **2004**, *19*, (9), 1045-1055.

787 41. Schuster, B.; Sleytr, U. B., Biomimetic interfaces based on S-layer proteins, lipid membranes and  
788 functional biomolecules. *J R Soc Interface* **2014**, *11*, (96).

789 42. Albers, S. V.; Meyer, B. H., The archaeal cell envelope. *Nat Rev Microbiol* **2011**, *9*, (6), 414-26.

790 43. Sleytr, U. B.; Egelseer, E. M.; Ilk, N.; Pum, D.; Schuster, B., S-layers as a basic building block in a  
791 molecular construction kit. *FEBS J* **2007**, *274*, 323-334.

792 44. Rodrigues-Oliveira, T.; Belmok, A.; Vasconcellos, D.; Schuster, B.; Kyaw, C. M., Archaeal S-Layers:  
793 Overview and Current State of the Art. *Front Microbiol* **2017**, *8*, (2597).

794 45. Whitman, W. B.; Coleman, D. C.; Wiebe, W. J., Prokaryotes: The unseen majority. *Proc Natl Acad Sci U  
795 S A* **1998**, *95*, 6578-6583.

796 46. Messner, P.; Schäffer, C.; Egelseer, E. M.; Sleytr, U. B., Occurrence, Structure, Chemistry, Genetics,  
797 Morphogenesis, and Function of S-Layers. In *Prokaryotic Cell Wall Compounds - Structure and  
798 Biochemistry*, König, H.; Claus, H.; Varma, A., Eds. Springer: Heidelberg, Germany, 2010; Vol. Chapter  
799 2, pp 53-109.

800 47. Sleytr, U. B., Heterologous reattachment of regular arrays of glycoproteins on bacterial surfaces.  
801 *Nature* **1975**, *257*, (5525), 400-2.

802 48. Sleytr, U. B.; Huber, C.; Ilk, N.; Pum, D.; Schuster, B.; Egelseer, E. M., S-Layers as a tool kit for  
803 nanobiotechnological applications. *FEMS Microbiol Lett* **2007**, *267*, 131-144.

804 49. Sleytr, U. B., Regular arrays of macromolecules on bacterial cell walls: structure, chemistry, assembly,  
805 and function. *Int Rev Cytol* **1978**, *53*, 1-62.

806 50. Sleytr, U. B.; Egelseer, E. M.; Ilk, N.; Messner, P.; Schäffer, C.; Pum, D.; Schuster, B.,  
807 Nanobiotechnological applications of S-layers. In *Prokaryotic Cell Wall Compounds - Structure and  
808 Biochemistry*, König, H.; Claus, H.; Varma, A., Eds. Springer: Heidelberg, Germany, 2010; pp 459-481.

809 51. Sleytr, U. B.; Messner, P., Self-assembly of crystalline bacterial cell surface layers (S-layers). In *Electron  
810 Microscopy of Subcellular Dynamics*, Plattner, H., Ed. CRC Press: Boca Raton, Florida, 1989; pp 13-31.

811 52. Sleytr, U. B.; Schuster, B.; Egelseer, E. M.; Pum, D.; Horejs, C. M.; Tscheliessnig, R.; Ilk, N.,  
812 Nanobiotechnology with S-Layer Proteins as Building Blocks In *Progress in Molecular Biology and  
813 Translational Science, Molecular Assembly in Natural and Engineered Systems*, Howorka, S., Ed. Elsevier  
814 Academic Press Inc.: Burlington, 2011; Vol. 103, pp 277-352.

815 53. Sleytr, U. B., *Curiosity and passion for science and art*. 2016; Vol. 7, p 1-488.

816 54. Pavkov-Keller, T.; Howorka, S.; Keller, W., The structure of bacterial S-layer proteins. In *Molecular  
817 Assembly in Natural and Engineered Systems*, Howorka, S., Ed. Elsevier Academic Press Inc.: Burlington,  
818 2011; Vol. 103, pp 73-130.

819 55. Sleytr, U. B.; Beveridge, T. J., Bacterial S-layers. *Trends Microbiol* **1999**, 7, (6), 253-60.

820 56. Picher, M. M.; Küpcü, S.; Huang, C. J.; Dostalek, J.; Pum, D.; Sleytr, U. B.; Ertl, P., Nanobiotechnology  
821 advanced antifouling surfaces for the continuous electrochemical monitoring of glucose in whole  
822 blood using a lab-on-a-chip. *Lab Chip* **2013**, 13, (9), 1780-1789.

823 57. Sára, M.; Pum, D.; Sleytr, U. B., Permeability and charge-dependent adsorption properties of the S-  
824 layer lattice from *Bacillus coagulans* E38-66. *J Bacteriol* **1992**, 174, (11), 3487-93.

825 58. Sára, M.; Sleytr, U. B., S-Layer proteins. *J Bacteriol* **2000**, 182, (4), 859-68.

826 59. Sleytr, U. B.; Messner, P., Crystalline bacterial cell surface layers (S-layers). In *Encyclopedia of*  
827 *Microbiology*, 3rd ed.; Schaechter, M., Ed. Academic Press/Elsevier Science: San Diego, 2009; Vol. 1, pp  
828 89-98.

829 60. Sleytr, U. B.; Messner, P.; Pum, D.; Sára, M., Crystalline bacterial cell surface layers (S-layers): from  
830 supramolecular cell structure to biomimetics and nanotechnology. *Angew Chem Int Ed* **1999**, 38, 1034-  
831 1054.

832 61. Sleytr, U. B.; Sára, M.; Pum, D.; Schuster, B.; Messner, P.; Schäffer, C., Self-assembly protein systems:  
833 microbial S-layers. In *Biopolymers. Polyamides and complex proteinaceous materials I*, Steinbüchel, A.;  
834 Fahnestock, S. R., Eds. Wiley-VCH: Weinheim, 2002; Vol. 1st Ed., pp 285-338.

835 62. Fagan, R. P.; Fairweather, N. F., Biogenesis and functions of bacterial S-layers. *Nat Rev Micro* **2014**, 12,  
836 (3), 211-222.

837 63. Sleytr, U. B.; Egelseer, E. M.; Pum, D.; Schuster, B., S-Layers. In *NanoBiotechnology: Concepts, Methods*  
838 and *Perspectives*, Niemeyer, C. M.; Mirkin, C. A., Eds. Wiley-VCH: Weinheim, Germany, 2004; pp 77-  
839 92.

840 64. Pum, D.; Messner, P.; Sleytr, U. B., Role of the S layer in morphogenesis and cell division of the  
841 archaebacterium *Methanocorpusculum sinense*. *J Bacteriol* **1991**, 173, (21), 6865-6873.

842 65. Engelhardt, H.; Peters, J., Structural Research on Surface Layers: A Focus on Stability, Surface Layer  
843 Homology Domains, and Surface Layer–Cell Wall Interactions. *J Struct Biol* **1998**, 124, (2), 276-302.

844 66. Sotiropoulou, S.; Mark, S. S.; Angert, E. R.; Batt, C. A., Nanoporous S-layer protein lattices. A  
845 biological ion gate with calcium selectivity. *J Phys Chem C* **2007**, 111, (35), 13232-13237.

846 67. Sleytr, U. B.; Györvary, E.; Pum, D., Crystallization of S-layer protein lattices on surfaces and  
847 interfaces. *Prog Organ Coat* **2003**, 47, 279-287.

848 68. Pum, D.; Sára, M.; Sleytr, U. B., Structure, surface charge, and self-assembly of the S-layer lattice from  
849 *Bacillus coagulans* E38-66. *J Bacteriol* **1989**, 171, (10), 5296-303.

850 69. Pum, D.; Sleytr, U. B., Large-scale reconstruction of crystalline bacterial surface layer proteins at the  
851 air-water interface and on lipids. *Thin Solid Films* **1994**, 244, 882-886.

852 70. Pum, D.; Weinhandl, M.; Hödl, C.; Sleytr, U. B., Large-scale recrystallization of the S-layer of *Bacillus*  
853 *coagulans* E38-66 at the air/water interface and on lipid films. *J Bacteriol* **1993**, 175, (9), 2762-2766.

854 71. Györvary, E. S.; Stein, O.; Pum, D.; Sleytr, U. B., Self-assembly and recrystallization of bacterial S-layer  
855 proteins at silicon supports imaged in real time by atomic force microscopy. *J Microsc* **2003**, 212, (Pt 3),  
856 300-6.

857 72. Tang, J.; Ebner, A.; Ilk, N.; Lichtblau, H.; Huber, C.; Zhu, R.; Pum, D.; Leitner, M.; Pastushenko, V.;  
858 Gruber, H. J.; Sleytr, U. B.; Hinterdorfer, P., High-affinity tags fused to S-layer proteins probed by  
859 atomic force microscopy. *Langmuir* **2008**, 24, (4), 1324-1329.

860 73. Tang, J.; Ebner, A.; Badelt-Lichtblau, H.; Völlenkle, C.; Rankl, C.; Kraxberger, B.; Leitner, M.; Wildling,  
861 L.; Gruber, H. J.; Sleytr, U. B.; Ilk, N.; Hinterdorfer, P., Recognition imaging and highly ordered

862 molecular templating of bacterial S-layer nanoarrays containing affinity-tags. *Nano Lett* **2008**, 8, (12),  
863 4312-4319.

864 74. Pum, D.; Sleytr, U. B., Anisotropic crystal growth of the S-layer of *Bacillus sphaericus* CCM 2177 at the  
865 air/water interface. *Colloid Surface A* **1995**, 102, 99-104.

866 75. Pum, D.; Sleytr, U. B., Monomolecular reassembly of a crystalline bacterial cell surface layer (S-layer)  
867 on untreated and modified silicon surfaces. *Supramol Sci* **1995**, 2, 193-197.

868 76. Sleytr, U. B.; Sára, M.; Pum, D.; Schuster, B., Crystalline bacterial cell surface layers (S-layers): A  
869 versatile self-assembly system. In *Supramolecular Polymers*, Second Edition ed.; Ciferri, A., Ed. Taylor  
870 & Francis Group: Boca Raton, 2005; pp 583-612.

871 77. Rothbauer, M.; Küpcü, S.; Sticker, D.; Sleytr, U. B.; Ertl, P., Exploitation of S-layer anisotropy: PH-  
872 dependent nanolayer orientation for cellular micropatterning. *ACS Nano* **2013**, 7, (9), 8020-8030.

873 78. Weygand, M.; Kjaer, K.; Howes, P. B.; Wetzer, B.; Pum, D.; Sleytr, U. B.; Lösche, M., Structural  
874 reorganization of phospholipid headgroups upon recrystallization of an S-layer lattice. *J Phys Chem B*  
875 **2002**, 106, (22), 5793-5799.

876 79. Weygand, M.; Schalke, M.; Howes, P. B.; Kjaer, K.; Friedmann, J.; Wetzer, B.; Pum, D.; Sleytr, U. B.;  
877 Lösche, M., Coupling of protein sheet crystals (S-layers) to phospholipid monolayers. *J Mater Chem*  
878 **2000**, 10, (1), 141-148.

879 80. Weygand, M.; Wetzer, B.; Pum, D.; Sleytr, U. B.; Cuvillier, N.; Kjaer, K.; Howes, P. B.; Lösche, M.,  
880 Bacterial S-layer protein coupling to lipids: X-ray reflectivity and grazing incidence diffraction  
881 studies. *Biophys J* **1999**, 76, (1 I), 458-468.

882 81. Comolli, L. R., Conformational Transitions Driving Lattice Growth at an S-Layer Boundary Resolved  
883 by cryo-TEM. *Biophys J* **2013**, 104, (2), 353A-353A.

884 82. Comolli, L. R.; Siegerist, C. E.; Shin, S. H.; Bertozzi, C.; Regan, W.; Zettl, A.; De Yoreo, J.,  
885 Conformational Transitions at an S-Layer Growing Boundary Resolved by Cryo-TEM. *Angew Chem  
886 Int Ed* **2013**, 52, (18), 4829-4832.

887 83. Sleytr, U. B.; Messner, P.; Pum, D.; Sára, M., Kristalline Zelloberflächen-Schichten prokaryotischer  
888 Organismen (S Schichten): von der supramolekularen Zellstruktur zur Biomimetik und  
889 Nanotechnologie. *Angew Chem* **1999**, 111, 1098-1120.

890 84. Schuster, B.; Sleytr, U. B., Nanotechnology with S-layer proteins. In *Methods in Molecular Biology*,  
891 Gerrard, J. A.; Gerrard, J. A., Eds. 2013; Vol. 996, pp 153-175.

892 85. Györvary, E. S.; O'Riordan, A.; Quinn, A. J.; Redmond, G.; Pum, D.; Sleytr, U. B., Biomimetic  
893 nanostructure fabrication: Nonlithographic lateral patterning and self-assembly of functional bacterial  
894 S-layers at silicon supports. *Nano Lett* **2003**, 3, (3), 315-319.

895 86. Schuster, B., Sleytr, U.B., The effect of hydrostatic pressure on S layer-supported lipid membranes.  
896 *Biochim Biophys Acta* **2002**, 1563, 29-34.

897 87. Schuster, B.; Sleytr, U. B., Biomimetic S-layer supported lipid membranes. *Curr Nanosci* **2006**, 2, (2),  
898 143-152.

899 88. Illk, N.; Egelseer, E. M.; Sleytr, U. B., S-layer fusion proteins-construction principles and applications.  
900 *Curr Opin Biotechnol* **2011**, 22, 824-831.

901 89. Moll, D.; Huber, C.; Schlegel, B.; Pum, D.; Sleytr, U. B.; Sára, M., S-layer-streptavidin fusion proteins  
902 as template for nanopatterned molecular arrays. *Proc Natl Acad Sci USA* **2002**, 99, (23), 14646-14651.

903 90. Ilk, N.; Schumi, C. T.; Bohle, B.; Egelseer, E. M.; Sleytr, U. B., Expression of an endotoxin-free S-  
904 layer/allergen fusion protein in gram-positive *Bacillus subtilis* 1012 for the potential application as  
905 vaccines for immunotherapy of atopic allergy. *Microb Cell Fact* **2011**, *10*, 6.

906 91. Ilk, N.; Küpcü, S.; Moncayo, G.; Klimt, S.; Ecker, R. C.; Hofer-Warbinek, R.; Egelseer, E. M.; Sleytr, U.  
907 B.; Sára, M., A functional chimaeric S-layer-enhanced green fluorescent protein to follow the uptake  
908 of S-layer-coated liposomes into eukaryotic cells. *Biochem J* **2004**, *379*, (Pt 2), 441-8.

909 92. Sára, M.; Egelseer, E. M.; Huber, C.; Ilk, N.; Pleschberger, M.; Pum, D.; Sleytr, U. B., S-layer proteins:  
910 Potential application in nano(bio)technology. In *Microbial Bionanotechnology: Biological Self-Assembly*  
911 *Systems and Biopolymer-Based Nanostructures*, Bernd Rehm Massey University, P. N., New Zealand, Ed.  
912 Horizon Bioscience: 2006; pp 307-338.

913 93. Schuster, B., Biomimetic design of nano-patterned membranes. *Nanobiotechnology* **2005**, *1*, 153-164.

914 94. Schuster, B.; Kepplinger, C.; Sleytr, U. B., Biomimetic S-layer stabilized lipid membranes. In  
915 *Biomimetics in Biophysics: model systems, experimental techniques and computation*, Toca-Herrera, J. L., Ed.  
916 Research Signpost: Kerala, India, 2010; pp 1-12.

917 95. Schuster, B.; Pum, D.; Sleytr, U. B., S-layer stabilized lipid membranes. *Biointerphases* **2008**, *3*, (2), FA3-  
918 FA11.

919 96. Schuster, B.; Sleytr, U. B., 2D-Protein Crystals (S-Layers) as Support for Lipid Membranes. In *Advances*  
920 *in Planar Lipid Bilayers and Liposomes*, Tien, T. H.; Ottova, A., Eds. Elsevier Science: Amsterdam, The  
921 Netherlands, 2005; Vol. 1, pp 247-293.

922 97. Schuster, B.; Sleytr, U. B., Composite S-layer lipid structures. *J Struct Biol* **2009**, *168*, 207-216.

923 98. Schuster, B., Pum, D., Sára, M., Sleytr, U.B., S-Layer Proteins as Key Components of a Versatile  
924 Molecular Construction Kit for Biomedical Nanotechnology. *Mini-Rev Med Chem* **2006**, *6*, 909-920.

925 99. Sleytr, U. B.; Pum, D.; Sára, M.; Schuster, B., Molecular nanotechnology and nanobiotechnology with  
926 2-D protein crystals. In *Encyclopedia of Nanoscience and Nanotechnology*, Nalwa, H. S., Ed. Academic  
927 Press: San Diego, 2004; Vol. 5, pp 693-702.

928 100. Sleytr, U. B.; Schuster, B.; Pum, D., Nanotechnology and biomimetics with 2D protein crystals (S-  
929 layers). *IEEE Eng Med Biol* **2003**, *22*, 140-150.

930 101. Clark, L. C., Jr.; Lyons, C., Electrode systems for continuous monitoring in cardiovascular surgery.  
931 *Ann NY Acad Sci*, **1962**, *102*, 29-45.

932 102. Chen, C.; Zhao, X. L.; Li, Z. H.; Zhu, Z. G.; Qian, S. H.; Flewitt, A. J., Current and emerging technology  
933 for continuous glucose monitoring. *Sensors* **2017**, *17* (1), E182.

934 103. Justino, C. I. L.; Duarte, A. C.; Rocha-Santos, T. A. P., Critical overview on the application of sensors  
935 and biosensors for clinical analysis. *Trends Anal Chem* **2016**, *85*, 36-60.

936 104. Mehrotra, P., Biosensors and their applications - A review. *J Oral Biol Craniofacial Res* **2016**, *6*, (2), 153-  
937 159.

938 105. Shende, P.; Sahu, P.; Gaud, R., A technology roadmap of smart biosensors from conventional glucose  
939 monitoring systems. *Ther Deliv* **2017**, *8*, (6), 411-423.

940 106. Hasanzadeh, M.; Shadjou, N., Electrochemical nanobiosensing in whole blood: Recent advances.  
941 *Trends Anal Chem* **2016**, *80*, 167-176.

942 107. Soleymani, J.; Perez-Guaita, D.; Hasanzadeh, M.; Shadjou, N.; Jouyban, A., Materials and methods of  
943 signal enhancement for spectroscopic whole blood analysis: Novel research overview. *Trends Anal*  
944 *Chem* **2017**, *86*, 122-142.

945 108. Sleytr, U. B.; Bayley, H.; Sára, M.; Breitwieser, A.; Küpcü, S.; Mader, C.; Weigert, S.; Unger, F. M.;  
946 Messner, P.; Jahn-Schmid, B.; Schuster, B.; Pum, D.; Douglas, K.; Clark, N. A.; Moore, J. T.;  
947 Winningham, T. A.; Levy, S.; Frithsen, I.; Pankovc, J.; Beale, P.; Gillis, H. P.; Choutov, D. A.; Martin, K.  
948 P., VI. Applications of S-layers. *FEMS Microbiol Rev* **1997**, *20*, (1-2), 151-175.

949 109. Sleytr, U. B.; Sára, M., Ultrafiltration membranes with uniform pores from crystalline bacterial cell  
950 envelope layers. *Appl Microbiol Biot* **1986**, *25*, (2), 83-90.

951 110. Sára, M.; Küpcü, S.; Weiner, C.; Weigert, S.; Sleytr, U. B., Crystalline protein layers as isoporous  
952 molecular sieves and immobilisation and affinity matrices. In *Immobilised Macromolecules: Application*  
953 *Potentials*, Sleytr, U. B.; Messner, P.; Pum, D.; Sára, M., Eds. Springer-Verlag: London, UK, 1993; pp 71-  
954 86.

955 111. Sára, M.; Manigley, C.; Wolf, G.; B., S. U., Isoporous ultrafiltration membranes from bacterial cell  
956 envelope layers. *J. Membr. Sci.* **1988**, *36*, 179-186.

957 112. Sára, M.; Sleytr, U. B., Production and characteristics of ultrafiltration membranes with uniform pores  
958 from two-dimensional arrays of proteins. *J. Membr. Sci.* **1987**, *33*, 27-49.

959 113. Park, T. J.; Lee, S. J.; Park, J. P.; Yang, M. H.; Choi, J. H.; Lee, S. Y., Characterization of a bacterial self-  
960 assembly surface layer protein and its application as an electrical nanobiosensor. *J Nanosci Nanotechno*  
961 **2011**, *11*, (1), 402-407.

962 114. Pum, D.; Neubauer, A.; Sleytr, U. B.; Pentzien, S.; Reetz, S.; Kautek, W., Physico-chemical properties  
963 of crystalline nanoscale enzyme-protein-metal layer composites in biosensors. *Ber Bunsen Phys Chem*  
964 **1997**, *101*, (11), 1686-1689.

965 115. Pum, D.; Sára, M.; Sleytr, U. B., Two-dimensional (glyco)protein crystals as patterning elements and  
966 immobilisation matrices for the development of biosensors. In *Immobilised Macromolecules: Application*  
967 *Potentials*, Sleytr, U. B.; Messner, P.; Pum, D.; Sára, M., Eds. Springer-Verlag: London, UK, 1993; pp  
968 141-160.

969 116. Sára, M.; Küpcü, S.; Weiner, C.; Weigert, S.; Sleytr, U. B., S-layers as immobilization and affinity  
970 matrices. In *Advances in bacterial paracrystalline surface layers*, Beveridge, T. J.; Koval, S. F., Eds. Plenum  
971 Press: New York & London, 1993; Vol. 252.

972 117. Neubauer, A.; Pum, D.; Sleytr, U. B., An amperometric glucose sensor based on isoporous crystalline  
973 protein membranes as immobilization matrix. *Anal Lett* **1993**, *26*, 1347-1360.

974 118. Neubauer, A.; Hödl, C.; Pum, D.; Sleytr, U. B., A multistep enzyme sensor for sucrose based on S-  
975 layer microparticles as immobilization matrix. *Anal Lett* **1994**, *27*, 849-865.

976 119. Neubauer, A.; Pum, D.; Sleytr, U. B., Fibre-optic glucose biosensor using enzyme membranes with 2-  
977 D crystalline structure. *Biosens Bioelectron* **1996**, *11*, 317-325.

978 120. Neubauer, A.; Pentzien, S.; Reetz, S.; Kautek, W.; Pum, D.; Sleytr, U. B., Pulsed-laser metal contacting  
979 of biosensors on the basis of crystalline enzyme-protein layer composites. *Sensor Actuator B-Chem*  
980 **1997**, *40*, (2-3), 231-236.

981 121. Schuster, B.; Sleytr, U. B., Relevance of glycosylation of S-layer proteins for cell surface properties.  
982 *Acta Biomater.* **2015**, *19*, 149-157.

983 122. Ferraz, H. C.; Guimarães, J. A.; Alves, T. L. M.; Constantino, C. J. L., Monomolecular films of  
984 cholesterol oxidase and S-Layer proteins. *Appl Surf Sci* **2011**, *257*, (15), 6535-6539.

985 123. Guimarães, J. A.; Ferraz, H. C.; Alves, T. L. M., Langmuir-Blodgett films of cholesterol oxidase and S-  
986 layer proteins onto screen-printed electrodes. *Appl Surf Sci* **2014**, *298*, 68-74.

987 124. Scheicher, S. R.; Kainz, B.; Köstler, S.; Suppan, M.; Bizzarri, A.; Pum, D.; Sleytr, U. B.; Ribitsch, V.,  
988 Optical oxygen sensors based on Pt(II) porphyrin dye immobilized on S-layer protein matrices.  
989 *Biosens Bioelectron* **2009**, 25, (4), 797-802.

990 125. Conroy, D. J. R.; Millner, P. A.; Stewart, D. I.; Pollmann, K., Biosensing for the environment and  
991 defence: Aqueous uranyl detection using bacterial surface layer proteins. *Sensors* **2010**, 10, (5), 4739-  
992 4755.

993 126. Egelseer, E. M.; Ilk, N.; Pum, D.; Messner, P.; Schäffer, C.; Schuster, B.; Sleytr, U. B., S-Layers,  
994 Microbial, Biotechnological Applications. In *The Encyclopedia of Industrial Biotechnology: Bioprocess,*  
995 *Bioseparation, and Cell Technology* Flickinger, M. C., Ed. John Wiley & Sons, Inc.: Hoboken, USA, 2010;  
996 Vol. 7, pp 4424-4448.

997 127. Huber, C.; Egelseer, E. M.; Ilk, N.; Sleytr, U. B.; Sára, M., S-layer-streptavidin fusion proteins and S-  
998 layer-specific heteropolysaccharides as part of a biomolecular construction kit for application in  
999 nanobiotechnology. *Microelectron Eng* **2006**, 83, 1589-1593.

1000 128. Huber, C.; J. Liu; E. M. Egelseer; D. Moll; W. Knoll; U. B. Sleytr; Sára, M., Heterotetramers formed by  
1001 an S-layer-streptavidin fusion protein and core-streptavidin as nanoarrayed template for biochip  
1002 development. *Small* **2006**, 2, 142-150.

1003 129. Pleschberger, M.; Neubauer, A.; Egelseer, E. M.; Weigert, S.; Lindner, B.; Sleytr, U. B.; Muyldermans,  
1004 S.; Sára, M., Generation of a functional monomolecular protein lattice consisting of an S-layer fusion  
1005 protein comprising the variable domain of a camel heavy chain antibody. *Bioconjug Chem* **2003**, 14, (2),  
1006 440-448.

1007 130. Pleschberger, M.; Saerens, D.; Weigert, S.; Sleytr, U. B.; Muyldermans, S.; Sára, M.; Egelseer, E. M., An  
1008 S-layer heavy chain camel antibody fusion protein for generation of a nanopatterned sensing layer to  
1009 detect the prostate-specific antigen by surface plasmon resonance technology. *Bioconjug Chem* **2004**,  
1010 15, (3), 664-671.

1011 131. Weber, V.; Ilk, N.; Völlenkle, C.; Weigert, S.; Sára, M.; Sleytr, U. B.; Falkenhagen, D., Extrakorporale  
1012 Blutreinigung mit spezifischen Absorbentien auf Basis der S-Schicht-Technologie. In *Medizin 2002-Aus*  
1013 *Forschung und Praxis*, Dézsy, J., Ed. Dr. Peter Müller Verlag: Wien, 2002.

1014 132. Völlenkle, C.; Weigert, S.; Ilk, N.; Egelseer, E.; Weber, V.; Loth, F.; Falkenhagen, D.; Sleytr, U. B.; Sára,  
1015 M., Construction of a functional S-layer fusion protein comprising an immunoglobulin G-binding  
1016 domain for development of specific adsorbents for extracorporeal blood purification. *Appl Environ*  
1017 *Microbiol* **2004**, 70, (3), 1514-1521.

1018 133. Tschiggerl, H.; Breitwieser, A.; de Roo, G.; Verwoerd, T.; Schäffer, C.; Sleytr, U. B., Exploitation of the  
1019 S-layer self-assembly system for site directed immobilization of enzymes demonstrated for an  
1020 extremophilic laminarinase from *Pyrococcus furiosus*. *J Biotechnol* **2008**, 133, (3), 403-11.

1021 134. Tschiggerl, H.; Casey, J. L.; Parisi, K.; Foley, M.; Sleytr, U. B., Display of a peptide mimotope on a  
1022 crystalline bacterial cell surface layer (S-layer) lattice for diagnosis of Epstein-Barr virus infection.  
1023 *Bioconjug Chem* **2008**, 19, (4), 860-5.

1024 135. Ferner-Ortner-Bleckmann, J.; Schrems, A.; Ilk, N.; Egelseer, E. M.; Sleytr, U. B.; Schuster, B.,  
1025 Multitechnique study on a recombinantly produced *Bacillus halodurans* laccase and an S-layer/laccase  
1026 fusion protein. *Biointerphases* **2011**, 6, (2), 63-72.

1027 136. Sprott, G.D., Yeung, A., Dicaire, C.J., Yu, S.H., Whitfield, D.M. Synthetic archaeosome vaccines  
1028 containing triglycosylarchaeols can provide additive and long-lasting immune responses that are  
1029 enhanced by archaetidylserine. *Archaea* **2012**, 513231.

1030 137. De Rosa, M., Archaeal lipids: Structural features and supramolecular organization. *Thin Solid Films*  
1031 1996, 284-285, 13-17.

1032 138. Hanford, M. J.; Peeples, T. L., Archaeal tetraether lipids: Unique structures and applications. *Appl*  
1033 *Biochem Biotech-A* 2002, 97, (1), 45-62.

1034 139. Engelhardt, H., Are S-layers exoskeletons? The basic function of protein surface layers revisited. *J*  
1035 *Struct Biol* 2007, 160, 115-124.

1036 140. Engelhardt, H., Mechanism of osmoprotection by archaeal S-layers: A theoretical study. *J Struct Biol*  
1037 2007, 160, 190-199.

1038 141. Schuster, B.; Pum, D.; Sleytr, U. B., Voltage clamp studies on S-layer-supported tetraether lipid  
1039 membranes. *Biochim Biophys Acta* 1998, 1369, (1), 51-60.

1040 142. Schuster, B.; Gufler, P. C.; Pum, D.; Sleytr, U. B., S-layer proteins as supporting scaffoldings for  
1041 functional lipid membranes. *IEEE Trans Nanobioscience* 2004, 3, (1), 16-21.

1042 143. Schuster, B.; Sleytr, U. B., S-layer-supported lipid membranes. *J Biotechnol* 2000, 74, (3), 233-54.

1043 144. Schuster, B.; Sleytr, U. B., Single channel recordings of  $\alpha$ -hemolysin reconstituted in S-layer-  
1044 supported lipid bilayers. *Bioelectrochemistry* 2002, 55, (1-2), 5-7.

1045 145. Wetzer, B.; Pfandler, A.; Györvary, E.; Pum, D.; Lösche, M.; Sleytr, U. B., S-layer reconstitution at  
1046 phospholipid monolayers. *Langmuir* 1998, 14, (24), 6899-6906.

1047 146. Schrems, A.; Kibrom, A.; Küpcü, S.; Kiene, E.; Sleytr, U. B.; Schuster, B., Bilayer lipid membrane  
1048 formation on a chemically modified S-layer lattice. *Langmuir* 2011, 27, (7), 3731-3738.

1049 147. Schrems, A.; Larisch, V. D.; Stanetty, C.; Dutter, K.; Damiati, S.; Sleytr, U. B.; Schuster, B., Liposome  
1050 fusion on proteinaceous S-layer lattices triggered via  $\beta$ -diketone ligand-europium(III) complex  
1051 formation. *Soft Matter* 2011, 7, (12), 5514-5518.

1052 148. Kepplinger, C.; Ilk, N.; Sleytr, U. B.; Schuster, B., Intact lipid vesicles reversibly tethered to a bacterial  
1053 S-layer protein lattice. *Soft Matter* 2009, 5, (2), 325-333.

1054 149. Krivanek, R.; Rybar, P.; Küpcü, S.; Sleytr, U. B.; Hianik, T., Affinity interactions on a liposome surface  
1055 detected by ultrasound velocimetry. *Bioelectrochemistry* 2002, 55, (1-2), 57-59.

1056 150. Mader, C.; Küpcü, S.; Sleytr, U. B.; Sára, M., S-layer-coated liposomes as a versatile system for  
1057 entrapping and binding target molecules. *Biochim Biophys Acta* 2000, 1463, (1), 142-150.

1058 151. Badelt-Lichtblau, H.; Kainz, B.; Völlenkle, C.; Egelseer, E. M.; Sleytr, U. B.; Pum, D.; Ilk, N., Genetic  
1059 engineering of the S-layer protein SbpA of *Lysinibacillus sphaericus* CCM 2177 for the generation of  
1060 functionalized nanoarrays. *Bioconj Chem* 2009, 20, (5), 895-903.

1061 152. Howorka, S.; Sára, M.; Wang, Y.; Kuen, B.; Sleytr, U. B.; Lubitz, W.; Bayley, H., Surface-accessible  
1062 residues in the monomeric and assembled forms of a bacterial surface layer protein. *J Biol Chem* 2000,  
1063 275, (48), 37876-37886.

1064 153. Tang, J.; Badelt-Lichtblau, H.; Ebner, A.; Preiner, J.; Kraxberger, B.; Gruber, H. J.; Sleytr, U. B.; Ilk, N.;  
1065 Hinterdorfer, P., Fabrication of highly ordered gold nanoparticle arrays templated by crystalline  
1066 lattices of bacterial S-layer protein. *ChemPhysChem* 2008, 9, (16), 2317-2320.

1067 154. Kiene, E. Potential and limitations of S-layer as support for planar lipid bilayers. Doctoral thesis.  
1068 University of Natural Resources and Life Sciences, Vienna, Vienna, 2011.

1069 155. Tang, J.; Ebner, A.; Kraxberger, B.; Badelt-Lichtblau, H.; Gruber, H. J.; Sleytr, U. B.; Ilk, N.;  
1070 Hinterdorfer, P., Mapping short affinity tags on bacterial S-layer with an antibody. *ChemPhysChem*  
1071 2010, 11, (11), 2323-2326.

1072 156. Moll, D.; Huber, C.; Schlegel, B.; Pum, D.; Sleytr, U. B.; Sára, M., S-layer-streptavidin fusion proteins  
1073 as template for nanopatterned molecular arrays. *Proc Nat Acad Sci USA* **2002**, 99, (23), 14646-14651.

1074 157. Györvary, E.; Wetzer, B.; B., S. U.; Sinner, A.; Offenhäusser, A.; Knoll, W., Lateral diffusion of lipids in  
1075 silane-, dextran-, and S-layer-supported mono- and bilayers. *Langmuir* **1999**, 15, 1337-1347.

1076 158. Nikolelis, D. P., Hianik, T., Krull, U.J., Biosensors based on thin lipid films and liposomes.  
*Electroanalysis* **1999**, 11, (1), 7-15.

1078 159. Gufler, P. C.; Pum, D.; Sleytr, U. B.; Schuster, B., Highly robust lipid membranes on crystalline S-layer  
1079 supports investigated by electrochemical impedance spectroscopy. *Biochim Biophys Acta* **2004**, 1661,  
1080 (2), 154-165.

1081 160. Schuster, B.; Pum, D.; Sára, M.; Braha, O.; Bayley, H.; Sleytr, U. B., S-layer ultrafiltration membranes: a  
1082 new support for stabilizing functionalized lipid membranes. *Langmuir* **2001**, 17, 499-503.

1083 161. Schuster, B.; Weigert, S.; D., P.; Sára, M.; B., S. U., New Method for Generating Tetraether Lipid  
1084 Membranes on Porous Supports. *Langmuir* **2003**, 19, 2392-2397.

1085 162. Sára, M.; Sleytr, U. B., Membrane Biotechnology: Two-dimensional Protein Crystals for Ultrafiltration  
1086 Purposes. In *Biotechnology*, Rehm, H. J., Ed. VCH: Weinheim, 1988; Vol. 6b, pp 615-636.

1087 163. Küpcü, S.; Sára, M.; Sleytr, U. B., Influence of covalent attachment of low molecular weight substances  
1088 on the rejection and adsorption properties of crystalline proteinaceous ultrafiltration membranes.  
*Desalination* **1993**, 90, 65-76.

1089 164. Weigert, S.; Sára, M., Ultrafiltration membranes prepared from crystalline bacterial cell surface layers  
1090 as model systems for studying the influence of surface properties on protein adsorption. *J Membr Sci*  
1091 **1996**, 121, 185-196.

1092 165. Weigert, S.; Sára, M., Surface modification of an ultrafiltration membrane with crystalline structure  
1093 and studies on interactions with selected protein molecules. *J Membr Sci* **1995**, 106, 147-159.

1094 166. Lohner, K., Prossnigg, F., Biological activity and structural aspects of PGLa interaction with  
1095 membrane mimetic systems. *Biochim Biophys Acta* **2009**, 1788, 1656-1666.

1096 167. Schuster, B., Sleytr, U.B., Nanotechnology with S-Layer Proteins. In *Protein Nanotechnology: Protocols,  
1097 Instrumentation and Applications*, 2nd edn, Gerrard, J. A., Ed. Humana Press, Springer Science+Business  
1098 Media: New York, 2013; Vol. 996, pp 153-175.

1099 168. Schrems, A., Larisch, V.D., Sleytr, U.B., Hohenegger, M., Lohner, K., Schuster, B., Insertion of an  
1100 Anionic Analogue of the Antimicrobial Peptide PGLa in Lipid Architectures including S-Layer  
1101 Supported Lipid Bilayers. *Curr Nanosci* **2013**, 9, 262-270.

1102 169. Chang, W. K.; Wimley, W. C.; Searson, P. C.; Hristova, K.; Merzlyakov, M., Characterization of  
1103 antimicrobial peptide activity by electrochemical impedance spectroscopy. *Biochim Biophys Acta* **2008**,  
1104 1778, (10), 2430-2436.

1105 170. Wimley, W. C., Hristova, K., Antimicrobial Peptides; Successes, Challenges and Unanswered  
1106 Questions. *J Membr Biol* **2011**, 239, 27-34.

1107 171. Jackman, J. A., Knoll, W., Cho, N.-J., Biotechnology applications of tethered lipid bilayer membranes.  
1108 *Materials* **2012**, 5, 2637-2657.

1109 172. Schuster, B.; Sleytr, U. B., Tailor-made crystalline structures of truncated S-layer proteins on  
1110 heteropolysaccharides. *Soft Matter* **2009**, 5, (2), 334-341.

1111 173. Trojanowicz, M., Miniaturized biochemical sensing devices based on planar lipid membranes.  
1112 *Fresenius J Anal Chem* **2001**, 372, 246-260.

1113

1114 174. Larisch, V.-D. Characterization of the ryanodine receptor 1 in model lipid membranes. Master Thesis,  
1115 University of Natural Resources and Life Sciences, Vienna, Austria, Vienna, Austria, 2012.

1116 175. Damiati, S.; Zayni, S.; Schrems, A.; Kiene, E.; Sleytr, U. B.; Chopineau, J.; Schuster, B.; Sinner, E. K.,  
1117 Inspired and stabilized by nature: ribosomal synthesis of the human voltage gated ion channel  
1118 (VDAC) into 2D-protein-tethered lipid interfaces. *Biomater Sci* **2015**, 3, (10), 1406-1413.

1119 176. Colombini, M., VDAC: The channel at the interface between mitochondria and the cytosol. *Mol Cell  
1120 Biochem* **2004**, 256-257, (1-2), 107-115.

1121 177. Colombini, M., VDAC structure, selectivity, and dynamics. *Biochim Biophys Acta* **2012**, 1818, (6), 1457-  
1122 1465.

1123 178. Colombini, M., The VDAC channel: Molecular basis for selectivity. *Biochim Biophys Acta* **2016**, 1863,  
1124 (10), 2498-2502.

1125 179. Colombini, M.; Blachly-Dyson, E.; Forte, M., VDAC, a channel in the outer mitochondrial membrane.  
1126 *Ion channels* **1996**, 4, 169-202.

1127 180. Komarov, A. G.; Deng, D.; Craigen, W. J.; Colombini, M., New insights into the mechanism of  
1128 permeation through large channels. *Biophys J* **2005**, 89, (6), 3950-3959.

1129 181. Lee, A. C.; Xu, X.; Colombini, M., The role of pyridine dinucleotides in regulating the permeability of  
1130 the mitochondrial outer membrane. *J Biol Chem* **1996**, 271, (43), 26724-26731.

1131 182. Rostovtseva, T. K.; Komarov, A.; Bezrukov, S. M.; Colombini, M., Dynamics of nucleotides in VDAC  
1132 channels: Structure-specific noise generation. *Biophys J* **2002**, 82, (1), 193-205.

1133 183. Zizi, M.; Forte, M.; Blachly-Dyson, E.; Colombini, M., NADH regulates the gating of VDAC, the  
1134 mitochondrial outer membrane channel. *J Biol Chem* **1994**, 269, (3), 1614-1616.

1135 184. Howard, A. D.; McAllister, G.; Feighner, S. D.; Liu, Q.; Nargund, R. P.; Van der Ploeg, L. H. T.;  
1136 Patchett, A. A., Orphan G-protein-coupled receptors and natural ligand discovery. *Trends Pharmacol  
1137 Sci* **2001**, 22, (3), 132-140.

1138 185. Howard, A. D.; Wang, R.; Pong, S. S.; Mellin, T. N.; Strack, A.; Guan, X. M.; Zeng, Z.; Williams Jr, D.  
1139 L.; Feighner, S. D.; Nunes, C. N.; Murphy, B.; Stair, J. N.; Yu, H.; Jiang, Q.; Clements, M. K.; Tan, C. P.;  
1140 McKee, K. K.; Hrenluk, D. L.; McDonald, T. P.; Lynch, K. R.; Evans, J. F.; Austin, C. P.; Caskey, C. T.;  
1141 Van Der Ploeg, L. H. T.; Liu, Q., Identification of receptors for neuromedin U and its role in feeding.  
1142 *Nature* **2000**, 406, (6791), 70-74.

1143 186. Choi, Y. H.; Han, H. K., Nanomedicines: current status and future perspectives in aspect of drug  
1144 delivery and pharmacokinetics. *J Pharm Investigig* **2018**, 48, (1), 43-60.

1145 187. Sala, M.; Diab, R.; Elaissari, A.; Fessi, H., Lipid nanocarriers as skin drug delivery systems: Properties,  
1146 mechanisms of skin interactions and medical applications. *Int J Pharmaceut* **2018**, 535, (1-2), 1-17.

1147 188. Dearling, J. L. J.; Packard, A. B., Molecular imaging in nanomedicine – A developmental tool and a  
1148 clinical necessity. *J Control Release* **2017**, 261, 23-30.

1149 189. Küpcü, S.; Sára, M.; Sleytr, U. B., Liposomes coated with crystalline bacterial cell surface protein  
1150 (S-layer) as immobilization structures for macromolecules. *Biochim Biophys Acta* **1995**, 1235, (2), 263-  
1151 269.

1152 190. Ücisinik, M. H.; Küpcü, S.; Breitwieser, A.; Gelbmann, N.; Schuster, B.; Sleytr, U. B., S-layer fusion  
1153 protein as a tool functionalizing emulsomes and CurcuEmulsomes for antibody binding and  
1154 targeting. *Colloids Surf B: Biointerfaces* **2015**, 128, 132-139.

1155 191. Ücisinik, M. H.; Küpcü, S.; Debreczeny, M.; Schuster, B.; Sleytr, U. B., S-layer coated emulsomes as  
1156 potential nanocarriers. *Small* **2013**, 9, (17), 2895-2904.

1157 192. Ücisik, M. H.; Sleytr, U. B.; Schuster, B., Emulsomes meet S-layer proteins: An emerging targeted drug  
1158 delivery system. *Curr Pharm Biotechnol* **2015**, *16*, (4), 392-405.